Development & Analysis of Microwave cavity and Magnetic shielding for Rubidium atomic clock

Thesis submitted in partial fulfillment of the requirement for the award of degree of

Master of Engineering

In

Electronics Instrumentation and Control Engineering

By

Satyendra Singh Raghuwanshi

(Roll No. 80751021)

Under the supervision of:

Mr. M.D.Singh, Sr. Lecturer
EIED, Thapar Univ. Patiala

Dr. G.M. Saxena (Scientist 'F')
National Physical Laboratory, New Delhi

ELECTRICAL AND INSTRUMENTATION ENGG. DEPARTMENT

THAPAR UNIVERSITY

JULY 2009

CERTIFICATE

This is to certify that my work presented in this thesis entitled **"Development & Analysis of Microwave cavity and Magnetic shielding for Rubidium atomic clock"** in partial fulfillment of the requirement for the award of the degree of **Master of Engineering in Electronics Instrumentation and Control Engineering at Thapar University, Patiala**, is an original record under supervision and guidance of **Mr. M.D. Singh** and **Dr. G.M. Saxena** The matter embodied in this report has not been submitted anywhere for the award of any degree.

Date: - 13-07-09

Satyendra Singh Raghuwanshi

Roll No. 80751021

It is certified that the above statement made by the student is correct to the best of our knowledge and belief.

Mr. M.D. Singh

Sr. Lecturer, EIED

(Supervisor)

Thapar University, Patiala

Dr. G.M. Saxena

Scientist F

(Supervisor)

National Physical Laboratory, New Delhi

14/7/09

Dr. Smarajit Ghosh

Professor & Head, EIED

Thapar University, Patiala

14/7

Dr. R.K Sharma

Dean of Academic Affairs

Thapar University, Patiala

ACKNOWLEDGEMENT

I owe my most sincere gratitude to the **Supreme power, My Guru**, **my father**, **my mother** and **my brother** who honest support and obstinate love give me energy to complete this work successfully and gave me untiring help during my difficult moments .They have always wanted the best for me and I admire my mother determination and sacrifice to put me through college.

I express my deep sense of gratitude to my supervisor **Dr.G.M.Saxena** for providing me an opportunity to work in Time & Frequency, NPL. His astonishing language skills and his clear vision of scientific content help me in tremendous manner. Words can hardly express my sense of gratitude to **Dr. R.K Sharma** Dean of Academic Affairs, Thapar University Patiala and **Dr. Smarajit Ghosh** HOD, EIED Thapar University Patiala to encouragement and invaluable support to do my thesis at NPL.

I want to express my deep sense of gratitude to my supervisor **Dr. M.D. Singh.** His wide knowledge and logical way of thinking have been of great value for me and his wonderful attitude help in my thesis work tremendously; his kindness, patience is much appreciable. I wish to express my sincere thanks to **Dr. P.Banerjee** (Acting Director & HOD of Time & Frequency Division, NPL), for permitting and providing the facilities necessary for carrying out thesis work at NPL and **Dr. A. Sen Gupta**, **Mr. S.P.Negi, Mr. Patel, Dr. S. S. Bawa**, **Dr. A. K. Aggarwal** Head HRD group, NPL, for their support and encouragement during the course of thesis work. I am extremely thankful to **Mrs. Arundhati Chatterjee, Mr. A. K. Suri, Miss Pranali Thorat and Mrs. Aditri** for their invaluable support and help. I want to express my heartfelt thanks to my most valuable friends **Miss Amanpreet Kaur and Mr. Rahul Kumar, Mr. Mukesh Kumar, Mr. Sachin Agrahari** and **Mr. Gouri Shanker Sharma**. In my hard times you pushed me always in the right direction only because of your inspiration i am going towards the successful completion of my M.Tech degree.

Date: 13-07-09 Satyendra Singh Raghuwanshi

Table of Contents

List of Figures

List of Tables

List of Abbreviations

1. Rb	Rubidium
2. CS	Cesium
3. H	Hydrogen
4. RCO	Resistor Capacitor Oscillator
5. LCO	Inductor Capacitor Oscillator
6. OX	Crystal Oscillator
7. OCXO	Oven controlled Crystal Oscillator
8. TCXO	Temperature compensated Crystal Oscillator
9. VCXO	Voltage Controlled Crystal Oscillator
10. DCXO	Digitally Compensated Crystal Oscillator
11. MCXO	Microcomputer compensated Crystal Oscillator
12. DUT	Device Under Test
13. VSWR	Voltage Standing Wave Ratio
14. CAE	Computer-Aided-Engineering
15. VNA	Vector Network Analyzer
16. RFS	Rubidium Frequency Standard
17. TE	Transverse Electric
18. TM	Transverse Magnetic

List of Appendices

ABSTRACT

The fabrication design of microwave cavity and the magnetic field shielding factor are two import considerations in designing the physics package of the Rubidium atomic clock. The microwave cavity mode selection and machining of the cavity are based on the specific application.

In this thesis we have discussed the development of microwave cavity in TE111 mode as the size is an important parameter. The cavity finish is another important aspect and software simulation plays central role in deciding the quality factor (Q) and uniformity of the field pattern. In atomic clock applications the tolerance limit are very small. In the work reported in this thesis these points have been addressed adequately. The magnetic shielding is also an important issue as the external magnetic field fluctuations can reduce the frequency stability. In the thesis various factors have been analyzed so that an optimum magnetic shielding factor may be realized.

INTRODUCTION

This work carried out at National Physical Laboratory, New Delhi. There are many time and frequency standards available but mainly Cesium and Rubidium atomic frequency standard are used on the application requirement. Rubidium (Rb) is a secondary frequency standard but far less complex compared to cesium and hydrogen frequency standards. Due to its very good short-term frequency stability and light weight it is widely used in experiments related to communication, satellite application, global positioning satellite, time keeping and other experiments requiring standard time and frequency signals.

In this thesis the designing aspects of the microwave cavity of TE111 mode for Rb atomic clock are discussed for 6.834 GHz. Aluminum (Al) alloy is used in the fabrication of the cavity as material supported to be non-magnetic. The tuning of the cavity is done using the tuning plunger. The microwave field is injected through a 2 mm diameter loop using SMA connector. The quality factor (Q) and the frequency tuning range are measured from the observations taken through vector network analyzer (VNA) unit. The details of the VNA are reported from VNA user manual for ready reference the smith chart is given for elucidatory the technical aspects of the cavity. Theoretical description for describing the cavity is included. The observation taken for deciding the resonant frequency, tuning range and Q have be tabulated and discussed under various conditions. The observations are consistent with the theoretical values. The introduction and features to Rb frequency standard over other frequency standards are discussed in chapter 1. The fundamental principle of VNA is discussed in chapter 2.

We get the final shape of microwave cavity after 5 cavities are developed and analyzed which is discussed in chapter 3. The magnetic shielding is discussed for multilayer of shields. The calculations of longitudinal and transverse shielding factor under various conditions have discussed in chapter 4. Finally the discussion on the basis of experiment results and conclusion of the thesis is discussed in chapter 5 and chapter 6.

Literature Survey

Time is taken as a standard since ancient times for many applications. Research papers are available on time and frequency standard since starting of 20 century. But the uses of the atomic clocks (Cs or Rb) as a standard for time and in other applications come in picture around 1950.

Paper related to the frequency standards had been studied from various peer reviewed journals and conferences. A brief survey is given here sectionwise.

Marek Jaworski and Marian W. Pospieszalski [1], (1979) proposed a new method of determination the field distribution and resonator frequency of the resonator. By this method the solution is obtained in a form of successive approximation converging to the exact solution for the TE011 mode. The proposed analytical method presented for the first time allows the determination the field distribution of cylindrical dielectric resonators with arbitrarily small error. Due to small errors, it can be used in the measurement of complex permittivity of low-loss microwave insulators.

Prof. M.S.Leong and Prof. P.S. Kooi [2], (1981) analyze the mode-matching technique of a dielectric coded cavity that has a configuration, which is more generalize and show that how the resonant frequency varies with dielectric cavity dimensions. The generalized form of a dielectric loaded resonator analyzed herein should find immediate applications in measurement of dielectric properties and the tuning of solid-state oscillators.

H.E.Williams and T.M.Kwon [3],(1983) proposed a design of 6.8 GHz rectangular microwave cavity design for use in Rubidium vapor cell frequency standards. The design consists of a rectangular cavity operating in the TE101 mode partially loaded with loss dielectric slab. This combines the desirable H-field uniformity of conventional cylindrical TE011 cavities with the reduced size of cylindrical TE111 cavities. Careful selection actually results in a substantially smaller resonator then TE111 cavities, yet without significant degradation of field uniformity.

Pierre Tremblay and Michel Tetu [4], (1984) present the performance of passive Rb frequency standard operated under various modes of microwave excitation such as TE011, TE111 or TE101. They studied that the resonance curve pattern, which depends not only on light intensity and the microwave power when atomic system parameters are held constant but also on the Area and the location of the Photo detector. He concludes that the long term frequency stability has been improved of a passive Rb frequency standard is evaluated through white frequency noise. This study also shows that there exists an optimum value for the short term frequency stability as a function of incident light intensity and microwave injected power and this frequency stability could be reduced by a miss-setting of these variables.

William J. Riley [5], (1984) describes the Rb frequency standard design objectives and approach as well as the test result obtained. He studies that the overall design approach has been to choose a configuration of RFS (Rubidium frequency standard) that favors the highest possible performance. The basic objective in the RFS development is to meet the stringent stability, reliability and radiation hardness requirements of the the NAVSTAR satellite. The general specifications choose a configuration that favors the highest possible performance. To ensure highest possible performance, the design utilizes a discrete filter cell arrangement to permit separate control of the optical pumping spectrum. This allows the light shift effect to be independently null and reduces in-homogeneities in the absorption.

Jovan Lebric and Darko Kejfez [6], (1988) proposed the Finite Integration Technique (FIT) for numerical solution of interior electromagnetic boundary problems with rotational symmetry and its ability so solve for resonance frequency, Quality Factor and a distribution for a user define number of modes in cylindrical cavities with arbitrary distribution of dielectric media. The gradual and proportional reduction of the media permittivity, called the mode evolution, enabled the observation of the dielectric's influence on electric and magnetic field distribution inside the cavity. It has been shown

that the position of a field vortex, relative to the dielectric body, is not always a reliable criterion for the mode classification.

M. Mohammad Tahri and D. Mirshekar syahkal [7], (1989) present a One dimensional Finite Element method for accurate determination of modes in dielectric loaded cylindrical cavities and calculate the resonant frequencies, H-vector variation formulation and minimize with respect the coefficients of the expended filled component. In this method spurious modes can be effectively removed from the spectrum of physical modes by adding a penalty term to the vibration expression imposing a divergent free magnetic field constraint. The technique is proved to be very versatile, accurate and computationally efficient, particularly when dielectrics are the same length as cavity.

E. Eltsufin and S.Fel [8], (1991) design a compact rectangular cylindrical dielectric filled 6.8 GHz microwave cavity for Rb frequency standard. Here the cavity in a TE101 mode where the field in the upper part compress due the dielectric slab and the field in the lower part are compressed due the cylindrical shape which compensate the influence of the glass cell. The small size of the cavity and its rectangular shape evaluated the design of a very compact physics-package, only 87 CC in volume and the new model of 500 CC, low power consumption, low warm up current and very low phase noise.

Lindo L. Lewis [9], (1991) present a comparison of different frequency standard, which may be useful in selecting device for various applications. He emphasized is on stability performance of the precision frequency standards as well some physical characteristics and cost consideration. The quartz crystal offer many advantages but due to its limited long term performance because of their susceptibility to environmental effects, especially temperature, acceleration and aging the requirement come of frequency standards like Rubidium, Cesium etc

D. Watts et. Al [10], (1996) studies the statistics for normally distributed data of Rb frequency standard for standardizing the setting of specification. The benefits of

standardizing the setting of specification are discussed and some proposals for a standard to setting the specifications of commercial atomic frequency standards. The statically methods can be use as a guide to set specification for atomic frequency standard and production cost can be reduced by using sample testing and static process control

Hosokawa Mizuhiko [11], (2003) presents the basic physics of the atomic frequency standard. In Atomic clocks and atomic frequency standards various quantum transitions are used and how these atomic clocks equipments work. He also discusses the energy level of atom, lifetime, quantum transition, radiation and the Rasmey resonance for the precise measurement of the transition frequency. He describe some of the elementary physics required to understand operational principles involved in atomic frequency standards.

C. Audoin [12], (2003) presents understanding how the Rubidium technology works including basic principle of operations, advanced physics package and advance of Rb standard over other standards. The presented physical package with integrating the filtering technique into a microwave cavity is greatly reduce the physics package volume without giving up short-and long- term stability performance. The key features of this physics package are the low power consumption, small size and weight, and minimal environmental sensitivity and mechanical ruggedness.

Andreas Bauch [13], (2003) studied the Cesium atomic clock function performance and mutual comparison of frequency standards based on the hyperfine transition in Cesium and now incorporating the technique of laser cooling. He gives an overview of currently available commercial cesium clocks and primary standards.

Yan wang et. Al [14], (2007) presented the design of a Downsize microwave cavity for Rubidium vapor cell frequency standard with an integrated filter absorption cell. He also describes the three simulations and mechanical structure of a dielectric loaded cavity

operated in the TE111 mode as a result of this compact design, the physics package volume reduced to the 38 cm^3 and the volume of whole device is 216 cm^3.

James Campro [15], (2007) studied the understanding of the atomic and chemical physics of the vapor cell atomic clock and the role of optical pumping, buffer gas as well as light shift. In modern vapor-cell clocks, the buffers gas pressure is thousands of times greater than what is needed for dick narrowing. One reason for the higher pressure is to protect the Rb atoms collisions with the bare glass walls of the resonance cell. Narrow atomic resonance requires not only the elimination of Doppler broadening, but also a long coherence time.

D.U.Guber etc. [16], (1979) presented the formula for longitudinal shielding effectiveness of N thin, closely spaced, concentric cylinders of high permeability material have been developed and experimentally tested. Shielding effectiveness was determined by the incrementally increasing the field in a specified direction while monitoring the internal field. Both longitudinal and transverse axial shielding effectiveness were determined using a fluxgate magnetometer with 0.1 nT resolutions.

Hence from these paragraphs the work on Rubidium Atomic frequency standard and cylindrical microwave cavity's magnetic and electric field pattern have been studied.
So far much work has been done in the area of Rubidium frequency standard. But still there is scope for designing of cylindrical microwave cavity with dominant mode, microwave coupling loop designing for excitation the dominant mode as well as the orientation of loop inside the cavity, downsize the microwave cavity and physics package, high magnetic shielding for the Rubidium atomic clock.

Problem Formulation

The designing of microwave cavity and the magnetic shielding for the physics package is very important to get the desired stability, life time and other feature of Rubidium atomic clock. For designing microwave cavity selection of type of microwave cavity and the cavity material must be proper and accurate because the microwave device analysis and development is very critical.

The magnetic shielding is also an important issue because the earth magnetic fluctuations affect the transitions of Rb atoms inside the cavity so that the shielding material must be of higher permeability and the shielding factor must be the order of 10^4 to achieve the frequency stability of 10^{-13}.

CHAPTER 1
INTRODUCTION TO TIME-STANDARDS

1.1 TIME

Time is a fundamental unit that can be observed and measured with a clock of mechanical, electrical, or other Physical nature. Dictionary definitions bring out some interesting points: time-A non-spatial continuum in which events occur in apparently irreversible succession from past through present to the future. An interval separating two points on this continuum, measured essentially by selecting a regularly recurring event, such as the sunrise, and counting the number of its recurrences during the interval of duration.

Time is one of the seven base physical quantities, and the second is one of seven base units defined in the International System of Units (SI). The definitions of many other physical quantities based upon the unit of time. The definition of second was earlier based on the earth's rotational rate or as a fraction of the tropical year. That changed in 1967 when the era of atomic time keeping formally began. The current definition of the SI second is:

The duration of 9,192,631,770 periods of the radiation corresponding to the transition between two Hyperfine levels of the ground state of the cesium-133 atom.

Frequency is the rate of a repetitive event. If T is the period of a repetitive event, then the frequency f is its reciprocal, $1/T$. Conversely, the period is the reciprocal of the frequency, $T = 1/f$. Since the period is a time interval expressed in seconds (s), it is easy to see the close relationship between time interval and frequency. The standard unit for frequency is the hertz (Hz), defined as events or cycles per second. The frequency of electrical signals is often measured in multiples of hertz, including kilohertz (kHz), megahertz (MHz), or gigahertz (GHz).

1.2 THE NEED OF TIME AND FREQUENCY STANDARDS

Everybody needs time for day to day work. If we stop and think about it, time and frequency standards are involved in one way or another in just about everything we do.

Time and frequency standards supply us with three basic types of information. The first type, *date and time-of-day*, tell us when something happened. Date and time-of-day can be used to record events, or to make sure that multiple events are *synchronized*, or happen at the same time. it's easy to think of ways we use date and time-of-day in our everyday lives. For example, we use date information to remind us when birthdays, anniversaries, and other holidays are scheduled to occur. Our wristwatches and wall clocks help us get to school and work on time. If we plan to meet a friend for dinner at 6 p.m., that's a simple example of synchronization. If our watches agree, we should both arrive at about the same time. Date and time-of-day information have other, more sophisticated uses as well. Fighter planes flying in a high-speed formation require synchronized clocks. If one banks or turns at the wrong time, it could result in a collision and loss of life. If you are watching a network television program, the local station has to be ready to receive the network feed (usually from a satellite), at the exact instant it arrives. This requires synchronization of the station and network clocks. The instruments used to detect and measure earthquakes, called seismographs, require synchronized clocks so that data collected at various locations can be compared and combined. Stock market transactions need to be synchronized so that the buyer and seller can agree upon the same price at the same time. A time error of just a few seconds could result in a large difference in the price of a stock. The electric power companies also need time synchronization. They use synchronized clocks throughout their power grids, so they can instantly transfer power to the parts of the grid where it is needed most. They also use synchronized clocks to determine the location of short circuit faults along a transmission line. The second type of information, *time interval*, tells us "how long" it takes for something to happen. We use time interval to state our age, or the amount of time we have been alive.

For example, the quartz watch on your wrist keeps time by counting the frequency of a quartz crystal designed to run at a frequency of 32,768 Hz. When the crystal has oscillated 32,768 times, the watch records that one second has elapsed. The station has to transmit on this frequency as accurately as possible, so that its signal does not interfere with the signals from other stations. Your television has to be able to pick out the channel 7 frequency from all the other available radio signals, so that you see the correct picture

on your screen. A high speed Internet connection might use something called a T1 line, which sends data at a frequency of 1,544,000 bits per second (1.544 MHz). And the computer that you use to connect to the Internet might run at a frequency faster than 1 GHz (one billion cycles per second). All of these applications require an *oscillator* that produces a specific frequency. This oscillator should be *stable*, which means that the frequency it produces stays the same (with only minor variations) over long time intervals. Accurate frequency is critical to today's communication networks. It shouldn't surprise you that the highest capacity networks run at the highest frequencies. In order to send data faster, we need stable oscillators situated throughout a network that all produce nearly the same frequency. The process of making multiple oscillators run at the same frequency is called *synchronization*. Of course, all three types of time and frequency information are very closely related. As we mentioned, the standard unit of time interval is the second. If we count seconds in an agreed upon fashion, we can calculate the date and the time-of-day. And if we count the number of events that occur during a second, we can measure the frequency. It's easy to see that the world depends heavily on time and frequency information, and that we rely on many millions of clocks and oscillators to keep time and produce frequency. To keep the world running smoothly, these devices need to be periodically compared to an internationally recognized standard. This comparison might be as simple as setting our watch or alarm clock to the correct minute, or adjusting the frequency of an atomic oscillator so it keeps time within a few nanoseconds per day. The Indian Standard Time (IST) and frequency standards maintained at NPL, New Delhi.

1.3 THE ROLE OF QUARTZ CRYSTAL OSCILLATORS

The Quartz crystal oscillator offer the best short-term stability, least expensive, smallest size and lower power consumption commercial frequency standards. But it has limited long-term stability because of their susceptibility to environmental effects, especially temperature, acceleration and aging. So that the long term stability of crystal oscillator is improved by locking to the atomic transition frequency of Rb.

The technology of quartz crystal oscillators has played a very important part in the development of atomic frequency standards. Instead of the requirements on its frequency stability being relaxed, because it is locked to an atomic resonance, these requirements have actually been raised, especially in the short-term region. This is dictated by the need for a very high spectral purity at the output of a high-order frequency multiplier, as well as by the requirement for obtaining the best control by the atomic transition, as for specific applications of the atomic frequency standards. It should be mentioned that improvements have been achieved recently in the short-term frequency stability of quartz crystal oscillators by extremely good electronic design, proper use of feedback and careful selection of circuit components further progress can be expected in the future. Unfortunately crystal oscillators are plagued with ageing and this varies from unit to unit. In crystal oscillators used in connection with atomic frequency standards, this drift is of the order of 1×10^{-10} per day. This ageing is suppressed when the quartz crystal frequency generator is properly slaved to the atomic transition.

The hydrogen, cesium and rubidium frequency standards are systems in which the frequency of a 5 MHz or 10 MHz quartz crystal oscillator is controlled via frequency synthesis and appropriate circuitry by the part of the device which is devoted to the observation of the atomic transition. The signals which are available for users, comprising nominal frequencies such as 1 Hz, 1 MHz or 5 MHz, are derived directly from the quartz Crystal frequency generator. This oscillator is phase locked in active atomic frequency standards, or frequency locked in passive ones. Conventional techniques of frequency control are normally used, but the quality of the design is of prime importance in order to achieve the ultimate performances, characteristic of the atomic resonance. The bandwidth of the feedback loop must be restricted to a value of the order of 1 to 10 Hz, in order to minimize the effect of noise in the observation of the atomic transition.

1.4 ATOMIC FREQUENCY STANDARDS AND ATOMIC CLOCKS

An atomic frequency standard is a device which has the very high frequency stability and accuracy (order of 10^{-13}) and whose basic resonant system is an atom or a molecule

undergoing a transition between two well defined hyperfine sublevels. The elements used in the devices most commonly at present are hydrogen, rubidium and cesium in which the transitions take place between two the hyperfine levels of their ground state. It is an $m_F = 1$, $m_F = 0$ magnetic dipole transition, whose frequency is, to first order, independent of the weak magnetic field normally applied. F is the hyperfine level.

An atomic clock delivers pulses at time intervals of one second. Therefore an atomic clock produces a time scale. World-wide comparison of atomic time scales enables the Bureau International de 1'Heure in Paris to build the International Atomic Time (TAI) Scale which, after the fixing of some agreed origin, permits the dating of an event with the highest possible precision.

An atomic clock is derived from a quartz crystal oscillator. However, a crystal oscillator's RF frequency ν_{xtal} depends on a number of environment factors, such as humidity, vibration, and radiation that can cause the clock to either speed up or slow down. In the atomic clock, ν_{xtal} is electronically tied to an atomic resonance, thereby transferring the stability of atomic structure to the clock's tick rate.

The nature of frequency standards involving transition frequencies in the microwave region. The work is in progress on frequency and time standards. A comparison of mainly commercially used atomic frequency standard [9] on the basis of stability, accuracy, stability specifications for several types crystal oscillators is given in table1.1 and additional information on physical characteristics of precision frequency standards is included in table 1.2

Table 1.1

Characteristics Comparison of different Frequency standard

Device	Stability Stability			Temperature dependence	Life time	Comments
	@1s	@1day	@1year			
RCO	–	–	–	1×10^{-3} (0^oc + 50^oc)	–	10% tuning range
LCO	–	2×10^{-4}	2×10^{-2}	3×10^{-3} (-400 to + 7^oc)	–	1×10^{-6} tolerance Possible
Xo	–	1×10^{-10} to 2×10^{-7}	$2x10^{-6}$ to $1x10^{-5}$	$1 \times 10^{-7}/^oc$ to $5 \times 10^{-6}/^oc$	3-20yr	–
TCXO	–	–	1×10^{-6}	$1x10^{-7}$to$2x\ 10^{-6}$ (0^oc to $+50^oc$)	>5 yr	Lifetime often limited by tuning Tuning range 1×10^{-2} to$5\ x10^{-8}$
DCXO	2×10^{-12}	1×10^{-9} to 2×10^{-8}	1×10^{-6}	$5\ x10^{-8}$ (0^oc to $+70^oc$)	>5 yr	–
MCXO	–	1×10^{-9}	–	2×10^{-8} (-55 to $+85^oc$)	–	–
Vcxo	–	–	–	$1x10^{-4}$ to$1x10^{-6}$ (0^oc to $+50^oc$)	–	–
Ocxo	$5\ x10^{-12}$ to $5\ x10^{-10}$	–	5×10^{-8} to $1x\ 10^{-6}$	$1 \times 10^{-10}/^oc$ to $5 \times 10^{-6}/^oc$	10-20yr	Usually single oven, proportional control
Oxco-STD	5×10^{-13} to 5×10^{-11}	5×10^{-10} to 5×10^{-9}	–	–	–	Usually double oven
Ocxo-sc	5×10^{-14}	2×10^{-11} to 1×10^{-10}	–	–	–	Warm-up time of hours
Rb	5×10^{-12} to 3×10^{-11}	1×10^{-13}	Drift of parts in 10^{-10} /yr	$4x10^{-11}$to$2x10^{-10}$ (0^oc to $+50^oc$	>5 yr	Warm-up time of minutes
Cs	5×10^{-12} to 6×10^{-12}	2×10^{-13} to 3×10^{-14}	1×10^{-13}	5×10^{-12} (0^oc to $+50^oc$)	up to 5 yr	Accuracy of $\pm 4x\ 10^{-12}$ to $\pm\ 3x\ 10^{-11}$
H(Passive)	1×10^{-14}	–	$<1x\ 10^{-12}$	–	–	–

Table 1.2

Physical Characteristics of Precision Frequency Standards

Device	Volume (cm3)	Weight (kg)	Nominal Power (Watts)	Cost in Rs (x1000)
Ocxo	36	0.04	0.45	_
Ocxo-STD	1×10^3	1	2 to 5	75 to 435
Rb	395 to 24,000	0.55 to 15.4	10 to 35	200 to 1900
Cs	4×10^4	20 to 30	30 to 100	1250 to 2300
H(Passive)	1×10^5	35	< 70	_

1.5 RUBIDIUM ATOMIC FREQUENCY STANDARD

Rubidium used as a secondary frequency standard but it has other advantage over the standards shown in table1.1 and table 1.2. It has very good short term frequency stability and is light weight and less complex compared to cesium and hydrogen frequency standards. Due to these advantages, it widely used in experiments related to communication, satellite application, global positioning system (GPS), time keeping and time synchronization and several other experiments requiring standard time and frequency signals. The block diagram shown below in the figure1.1.

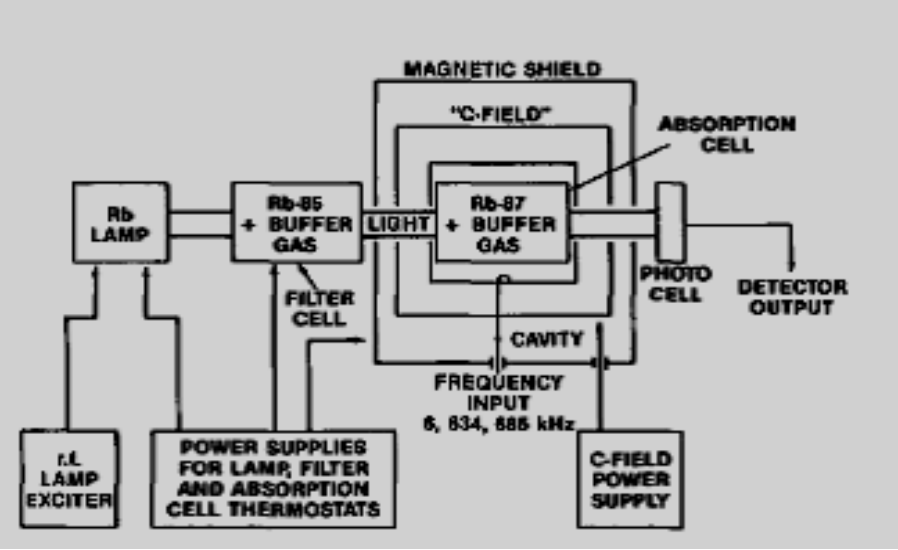

Fig.1.1 Block diagram of Rubidium atomic clock

1.6 PRINCIPLE

The Rb atomic frequency standard works on the principle, of phase locking a voltage controlled oscillator (VCXO) to the frequency of transitions between the ground state hyperfine sublevels F=2, $m_f = 0$ and F=1, $m_f = 0$ of Rb^{87} isotope as shown in the figure1.2 [8] These levels are chosen as they have second order dependence on magnetic field, to obtain the necessary correction signal for phase locking VCXO, the optical pumping technique is used for creating the population inversion between these hyperfine levels.

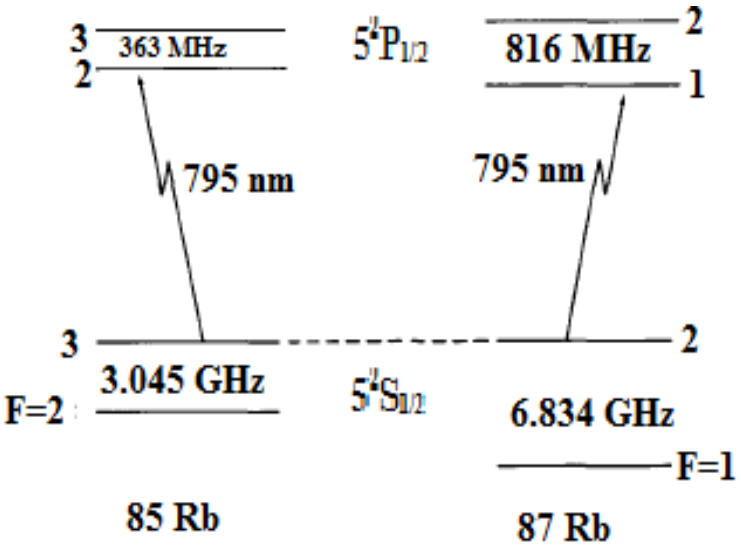

Figure 1.2 Energy level diagram for an Rb^{85} and Rb^{87}

In this technique, the light from an Rb^{87} lamp after filtering through an Rb^{85} filter cell, due to natural coincidence of optical resonance frequencies between Rb^{85} and Rb^{87} i.e. the hyperfine F=2 level of Rb^{87} and F=3 level of $Rb^{85}$of ground state overlap, is incident on an Rb^{87} absorption cell kept inside a microwave cavity tuned to the hyperfine transition frequency 6.834 GHz. As a result the filter light, with almost no transition from F=2 level to P excited states of Rb^{87} atoms, induces transitions from only F=1, ground state sublevel to the excited P levels. While relaxing back to the ground state, atoms have almost equal probability to occupy F=1 and F=2 levels. Thus the population of the F=2 level is increased while after sometime F=1 is completely depleted and a steady state with population inversion is obtained. The Rb^{85} absorption cell becomes more transparent to incident light. In this state of population inversion application of the resonant field microwave magnetic field in the direction of the light axis results in a net transition of atoms from F=2 to F=1 level and for restoring the steady, more light is absorbed in the Rb^{87} absorption cell. The transmitted light shows a dip in the intensity of the resonance signal monitored by a photovoltaic cell shown in figure1.3 [15] If the resonance microwave signal (i.e. microwave field) is phase modulated then resonance signal will show a composite nature containing the first and second harmonics riding on d.c. signal.

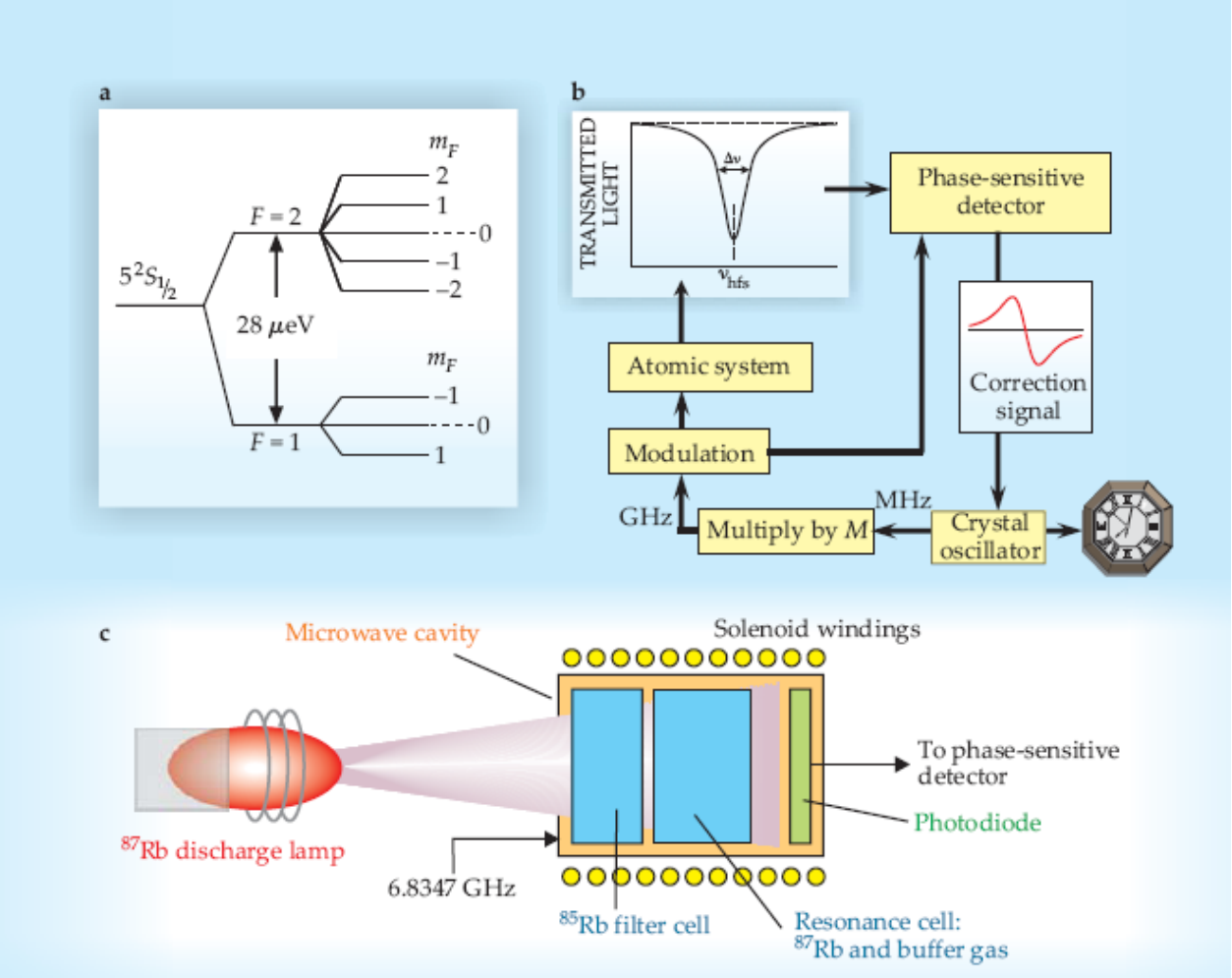

Figure1.3. (a) The ground states of Rb^{87} (b) The frequency locking of VCXO using phase sensitive detection (c) The optical pumping by Rb lamplight [15].

The resonant signal after phase sensitive detection and passing through a low pass filter produces a d.c. correction signal which is applied to electronic frequency control of VCXO. In this way the stability of the ground state hyperfine transition frequency is transferred to VCXO and the VCXO output of very high frequency stability is realized.

1.7 PHYSICS PACKAGE

The heart of the Rb frequency standard is a physics package where the atomic transitions take place. The physics package consists of following parts as shown in figure1.4.

- Rb lamp
- Absorption cell in integrated and separate configuration
- Microwave cavity
- Magnetic shielding
- Photo-detector for the atomic resonance

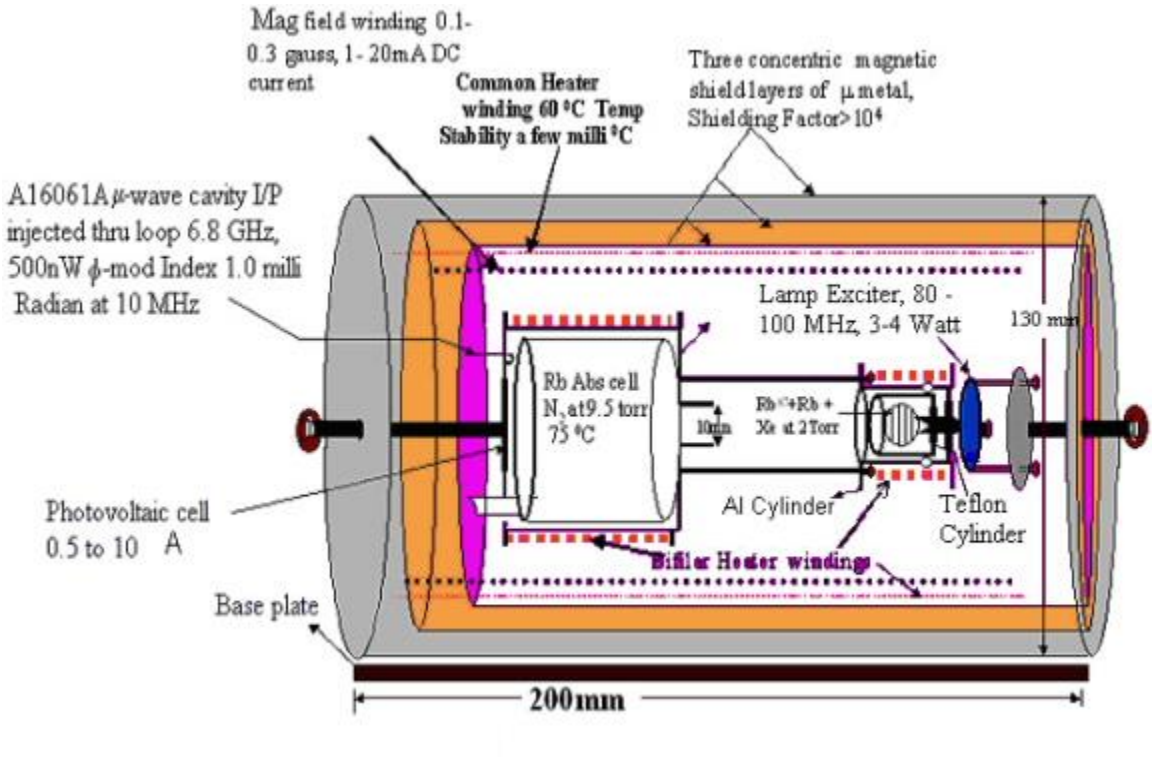

Figure 1.4 Physics package

1.7.1 Rb Lamp

Rb lamp consists of electrode less Rb bulb and a lamp exciter. Rb bulb made of pyrex glasses in spherical shape. The cylindrical bulb may also be used. The bulb is filled with Rb^{87}isotope and natural Rb in the 1:1 ratio and each in quantity of 0.35 mg. The use of mixer of natural and Rb^{87}in equal quantity provides minimization of the light shift.

The bulb filled with Xenon gas at 2 ± 0.2 Torr. The bulb is excited by 80-100 MHz/3-4 Watt RF exciter which is a colpitt's oscillator with a DC power supply of rating 15 Volt – 24 Volt and 0.2 – 0.4 Ampere current. Basic lamp exciter circuit [3] shown in figure1.5.

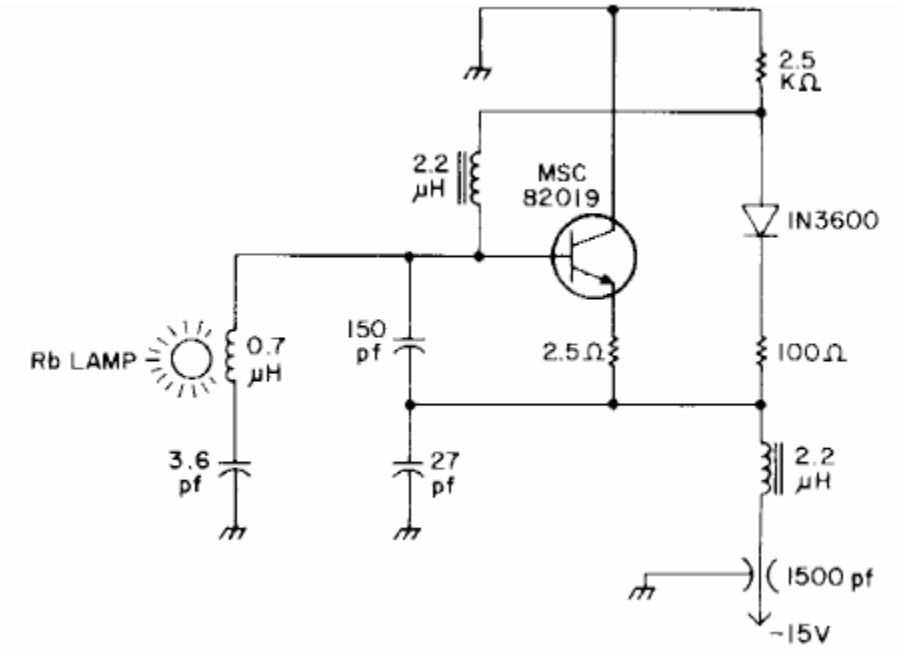

Fig.1.5 Basic lamp exciter circuit

The Rb discharge lamp not only drives the optical-pumping process but also provides a signal that indicates when the microwave field on resonance with m_f = 0-0 transition. When the field is off resonance, there are few atoms in the F=1 state, so most of the light passes through the resonance cell unabsorbed. But when the microwave frequency equals ν_{hfs} (hyperfine splitting frequency), the atoms returns to the F=1 state, and the intensity of the transmitted lamplight measured by the photodiode decreases.

1.7.2 Optical Pumping and Population Inversion

Optical pumping is a process in which light is used to raise (or "pump") electrons from a lower energy level in an atom or molecule to a higher one. It is commonly used in laser construction, to pump the active laser medium so as to achieve population inversion.

Optical pumping is also used to cyclically pump electrons bound within an atom or molecule to a well-defined quantum state. For the simplest case of coherent two-level optical pumping of an atomic species containing a single outer-shell electron, this means that the electron is coherently pumped to a single hyperfine sublevel which is defined by the polarization of the pump laser along with the quantum selection rules. Upon optical pumping, the atom is said to be *oriented* in a particular sublevel, however due to the cyclic nature of optical pumping the bound electron will actually be undergoing repeated excitation and decay between upper and lower state sublevels. The frequency and polarization of the pump laser determines which sublevel the atom is oriented in. For the Rb atomic frequency standard the optical pumping shown in figure1.3(c).

1.7.3 Absorption cell

The Rb absorption cell is a important part of physical package where the Rb hyperfine atomic transitions take place. These hyperfine transitions are primarily determining the frequency stability and other characteristics of the Rb atomic clock. The integrated cell filled with suitable mixture of $Rb^{87}$and Rb^{85}isotopes. The integrated technique is used to filtering of undesired transitions and also the excitation of the desired hyperfine transitions. It is observed from the experience and various experiments the desired filtering action may be achieved by using the natural Rb instead of adding $Rb^{87}$and Rb^{85} isotopes. A quantity of 1.5 to 2.0 mg is sufficient for the long life of the absorption cell. Further in order to achieve zero light shifts and to minimize the collision of atoms with wall, i.e. reduction in the speed of diffusion of atoms to a few cm/s, buffer gases are used.

Buffer gases such as He, N_2 and Ne produce positive frequency shifts of the microwave resonance. Heavier atoms such as Ar, Kr and Xe produce negative frequency shifts. Both the negative and positive shifts vary linearly in magnitude with the buffer gas pressure. Mixture of gases can be chosen to produce shifts which are very nearly zero. In our case Nitrogen (N_2) used as a buffer gas at 9.5 Torr pressure. The nitrogen gas has found to be very efficient for quenching the scattered radiation which would lower the efficiency of optical pumping. This property of N_2 helps in preventing radiation trapping which tends to effect the efficient optical pumping of Rb atoms.

Alkali metals are notorious for reabsorbing their fluorescent photons in a process known as radiation trapping [15], which has the effect of undoing the optical pumping effect of the lamp light. It's as if there were an extra source of light in the resonance cell that could excite atoms out of the Rb^{87} F=2 hyperfine level. But the radiation trapping can be avoided with the addition of N_2 as a buffer gas. When a Rb atom collides with a molecule of N_2, Rb electronic energy is converted into N_2 vibration energy, and the Rb atoms returns to its ground state without fluorescing. In this way very efficient optical pumping is relies in absorption cell.

1.7.4 Microwave Cavity

The integrated filter cell is kept inside the microwave cavity for excitation process of Rb atoms. An aluminum (Alloy of Al) cylindrical microwave cavity tuned at 6.835 GHz is used for exciting Rb ground states the hyperfine transition. One end of cavity is closed where the microwave signal feed through a loop and another end is open with threaded tunable plunger. This Plunger is used with a though hole of diameter such that the Rb lamp light effectively reached to the integrated filter cell. The absorption cell completely fills the microwave cavity. For the detection of resonance signal a photovoltaic cell kept at closed end i.e. at the end opposite to the plunger end. The microwave signal has its magnetic field is in the direction of the optical axis. This requirement for exciting the transitions between F=2, $m_f = 0$ to F=1, $m_f = 0$ of Rb^{87} isotope which have second order dependence on the magnetic field. On the outer surface of cylindrical cavity the bifilar heater winding for maintaining the temperature of the microwave cavity and cell at 75^oC. The required microwave power P is given by the expression

$$P = \frac{h^2 \omega_0 V_c b^2}{2\pi^2 \mu_0 \mu_b \eta Q_c} \qquad (1.1)$$

Where *h* the plank's constant, ω_0 is the Rf frequency, V_c is the cavity volume, b is the Rabi frequency, μ_0 is the permeability, μ_b is the Bohr Magneton, η is the filling factor and Q_c is the loaded quality factor of the cavity. Cavity designing, type and the mode of the cylindrical cavity in detailed is discussed in chapter 3.

1.7.5 The Role of DC Magnetic Field

The DC magnetic field is necessary to give an axis of quantization to the system and to adjust the frequency of the resonance cell to a value compatible with synthesizer used. It is produced either by a solenoid or by Helmholtz coils symmetrically situated relative to the resonance cell. In passive rubidium standards, magnetic field in-homogeneities do not affect the resonance signal much, since the atomic motion is inhibited by the buffer gas. In such case the broadening of the field-independent (0-0) transition is essentially inhomogeneous and is small. The broadening is more important for the field-dependent lines and field in-homogeneities reduce their intensity significantly. This may desirable condition, since upon turn-on the whole system should have fewer tendencies to lock to one of those field-dependent lines.

Since the resonance frequency of the rubidium standard is an intrinsic property of the Rb^{87}atom, the device is relatively free of the environmental perturbations. Frequency shifts must come from effects which alter the individual atoms, such as magnetic fields, or atomic collisions with the buffer gas, the magnetic field dependence of the resonance frequency of the rubidium microwave transition is given[9] by

$$f = 6834682613 + 574\ H^2 \qquad (1.2)$$

Where f is the frequency in hertz and H is the magnetic field is in oersted.

Because of this field dependence, the standard must be shielded from change in the earth's field, from power transformers, and other magnetic objects. The magnetic shielding for our case discuss in detailed in chapter 4.

1.7.6 Magnetic shielding

Magnetic interference is caused by the low impedance field sources such as transformer, power supplies, motor and AC lines.

The theoretical approach can be used to requiring field strength which is measured in oersteds and field density measure in Gauss or Tesla (Tesla = 10^4 Gauss). The formula for flux density is

$$B = \frac{1.25 \times D \times H_0}{t} \qquad (1.3)$$

Where B is the flux density in the shield material (in Gauss), D is diameter of diagonal of the shield in inches, H_0 ambient or source field in Gauss and t is the thickness of the shield in inches. The hyperfine transitions are very sensitive to the fluctuations in the external magnetic field. In order to protect the Rb absorption cell and other parts of the physics package from the magnetic field fluctuations three cylindrical layer of magnetic shield of high magnetic permeability are used. The CO-NETIC material, that has a very high magnetic attenuation and medium permeability 3 x 10^4, is used. To achieve the frequency fluctuations of less than 10^{-13} a shielding factor of the order of 10^4 is required. The shielding factor calculation Rb physics package for different dimensions is discussed in detailed in chapter 4.

After manufacturing is completed, hydrogen annealing will provide maximum permeability and attenuation. If skipping the annealing process seems tempting, remember that annealing approximately squares of the attenuation. Annealing often changes shield dimensions, so close tolerances that will add to the cost, and possibly require extensive tooling, should be avoided. Hence for efficient shielding the magnetic shield should be carefully Hydrogen annealed after fabrication.

1.7.7 Photo-detector

To detect the hyperfine transitions and to obtain the clock signal a photovoltaic cell with high efficiency in the near infrared (800 nm) is used. In the present case the detector is supposed to have large surface area covering the cross-sectional area of the absorption cell.

CHAPTER 2
INTRODUCTION TO VECTOR NETWORK ANALYZER

2.1 RF NETWORK ANALYZER

RF network analyzers are used for measuring a variety of components ranging from filters and frequency sensitive networks, to devices such as transistors, mixers and any RF orientated device. Typically RF network analyzers are more usually associated with microwave type frequencies. However the RF network analysers that are available cover down to much lower frequencies than this, and some are even able to make measurements at frequencies down to 1 Hz.

2.2 TYPES OF RF NETWORK ANALYZER

Within the broad scope of RF network analyzers, there are various types of instrument which can be bought and used. These types of RF network analyzer are very different, but they are all able to measure the parameters of RF components and devices but in different ways:

2.2.1 Scalar network analyzer (SNA)

The scalar network analyzer, SNA is a form of RF network analyzer that only measures the amplitude properties of the device under test, and in view of this it is the simpler of the various types of analyser. Effectively, a scalar network analyzer, SNA, works just as a spectrum analyzer in combination with a tracking generator. When a tracking generator and spectrum analyser are used together, their operation is electrically closely linked. scalar network analyzers, SNA, are very useful for measuring the amplitude response of a variety of components.

2.2.2 Vector network analyzer (VNA)

The vector network analyzer, VNA is a more useful form of RF network analyzer than the SNA as it is able to measure more parameters about the device under test. Not only does it measure the amplitude response, but it also looks at the phase as well. As a result vector network analyzer, VNA may also be called a gain-phase meter or an Automatic Network Analyzer. It is able to measure a variety of different parameters including the

amplitude response as well as the network scattering parameters, or S-parameters, which are the transmission and reflection coefficients for the device under test. These S-parameters contain both amplitude and phase information, and therefore a vector network analyzer, VNA is able to give a very comprehensive view of the device. In other words Vector network analysis is a method of accurately characterizing such components by measuring their effect on the amplitude and phase of swept-frequency and swept power test signals.

2.2.3 Large Signal Network Analyzer (LSNA):

The large signal network analyzer, LSNA is a highly specialized for of RF network analyzer that is able to investigate the characteristics of devices under large signal conditions. It is able to look at the harmonics and non-linearity's of a network under these conditions, providing a full analysis of its operation. A previous version of the Large Signal Network Analyzer, LSNA was known as the Microwave Transition Analyzer, MTA.

2.3 Difference between RF network analyzers and spectrum analyzers

Although there are many similarities between network analyzers and spectrum analyzers, there are also several major differences, especially in the types of measurements that are made. In particular they make very different types of measurement. In the first instance a spectrum analyzer is intended for analyzing the nature of signals that are fed into them. A network analyzer on the other hand generates a signal and uses this to analyze a network or device.

RF Network analyzers are used to measure components, devices, circuits, and sub-assemblies. An RF network analyzer will contain both a source and multiple receivers. It will display amplitude and often phase information (frequency or power sweeps) and normally in a ratio format. An RF network analyzer looks for a known signal, i.e. a known frequency, at the output of the device under test, since it is a stimulus response system. With vector-error correction, network analyzers provide much higher measurement accuracy than spectrum analyzers.

By contrast to RF network analyzers, spectrum analyzers are normally used to measure the characteristics of a signal rather than a device. The parameters measured may include: signal or carrier level, sidebands, harmonics, phase noise, etc. They are most commonly configured as a single channel receiver, without a source. Because of the flexibility needed to analyze signals, spectrum analyzers generally have a much wider range of IF bandwidths available than most RF network analyzers.

Spectrum analyzers can be used for testing networks such as filters. To achieve this they need tracking generator. When used in this way, spectrum analyzers can be used for scalar component testing (magnitude versus frequency, but no phase measurements). With spectrum analyzers, it is easy to get a trace on the display, but interpreting the results can be much more difficult than with a network analyzer.

2.4 PRINCIPLE OF VECTOR NETWORK ANALYZER

The fundamental principles of vector network analysis will be reviewed. The discussion includes the common parameters that can be measured, including the concept of scattering parameters (S-parameters). RF fundamentals such as transmission lines and the Smith chart will also be reviewed.

2.4.1 Importance of Vector Measurements

Measuring both magnitude and phase of components is important for several reasons. First, both measurements are required to fully characterize a linear network and ensure distortion-free transmission. To design efficient matching networks, complex impedance must be measured. Engineers developing models for computer-aided-engineering (CAE) circuit simulation programs require magnitude and phase data for accurate models.

In addition, time-domain characterization requires magnitude and phase information in order to perform an inverse-Fourier transform. Vector error correction, which improves measurement accuracy by removing the effects of inherent measurement-system errors, requires both magnitude and phase data to build an effective error model. Phase-measurement capability is very important even for scalar measurements such as return loss, in order to achieve a high level of accuracy.

2.4.2 The Basis of Incident and Reflected Power

In its fundamental form, network analysis involves the measurement of incident, reflected, and transmitted waves that travel along transmission lines. Using optical wavelengths as an analogy, when light strikes a clear lens (the incident energy), some of the light is reflected from the lens surface, but most of it continues through the lens (the transmitted energy) (Figure 2.1). If the lens has mirrored surfaces, most of the light will be reflected and little or none will pass through it. While the wavelengths are different for RF and microwave signals, the principle is the same. Network analyzers accurately measure the incident, reflected, and transmitted energy, e.g., the energy that is launched onto a transmission line, reflected back down the transmission line toward the source (due to impedance mismatch), and successfully transmitted to the terminating device (Such as an antenna).

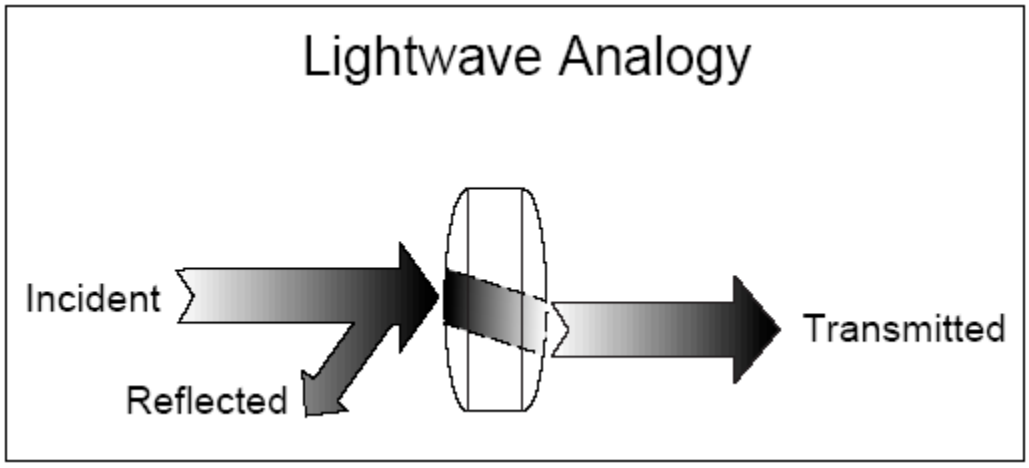

Fig.2.1 Light wave analogy to High-frequency device characterization

2.4.3 The Smith Chart

The amount of reflection that occurs when characterizing a device depends on the impedance that the incident signal "sees." Since any impedance can be represented with real and imaginary parts (R+jX or G+jB), they can be plotted on a rectilinear grid known

as the complex impedance plane. Unfortunately, an open circuit common RF impedance) appears at infinity on the real axis, and therefore cannot be shown. The polar plot is useful because the entire impedance plane is covered. However, instead of plotting impedance directly, the complex reflection coefficient is displayed in vector form. The magnitude of the vector is the distance from the center of the display, and phase is displayed as the angle of vector referenced to a flat line from the center to the right-most edge. The drawback of polar plots is that impedance values cannot be read directly from the display. Since there is a one-to-one correspondence between complex impedance and reflection coefficient, the positive real half of the complex impedance plane can be mapped onto the polar display. The result is the Smith chart. All values of reactance and all positive values of resistance from 0 to infinity fall within the outer circle of the Smith chart (Figure 2.2). On the Smith chart, loci of constant resistance appear as circles, while loci of constant reactance appear as arcs. Impedances on the Smith chart are always normalized to the characteristic impedance of the component or system of interest, usually 50 ohms for RF and microwave systems and 75 ohms for broadcast and cable-television systems. A perfect termination appears in the center of the Smith chart.

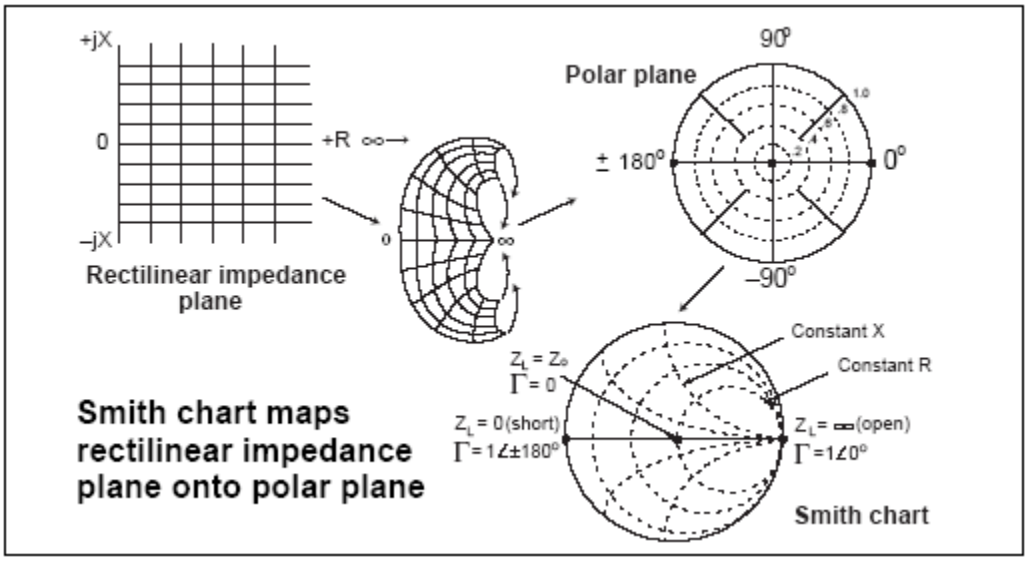

Fig.2.2 Smith chart review

2.4.4 Power Transfer Conditions

A perfectly matched condition must exist at a connection between two devices for maximum power transfer into a load, given a source resistance of RS and a load resistance of RL. This condition occurs when RL = RS, and is true whether the stimulus is a DC voltage source or a source of RF sine waves (Figure 2.3). When the source impedance is not purely resistive, maximum power transfer occurs when the load impedance is equal to the complex conjugate of the source impedance. This condition is met by reversing the sign of the imaginary part of the impedance. For example, if RS = 0.6 + j 0.3, then the complex conjugate is RS* = 0.6 – j 0.3. The need for efficient power transfer is one of the main reasons for the use of transmission lines at higher frequencies. At very low frequencies (with much larger wavelengths), a simple wire is adequate for conducting power. The resistance of the wire is relatively low and has little effect on low-frequency signals. The voltage and current are the same no matter where a measurement is made on the wire. At higher frequencies, wavelengths are comparable to or smaller than the length of the conductors in a high-frequency circuit, and power transmission can be thought of in terms of traveling waves. When the transmission line is terminated in its characteristic impedance, maximum power is transferred to the load. When the termination is not equal to the characteristic impedance, that part of the signal that is not absorbed by the load is reflected back to the source. If a transmission line is terminated in its characteristic impedance, no reflected signal occurs since all of the transmitted power is absorbed by the load (Figure 2.4). Looking at the envelope of the RF signal versus distance along the transmission line shows no standing waves because without reflections, energy flows in only one direction.

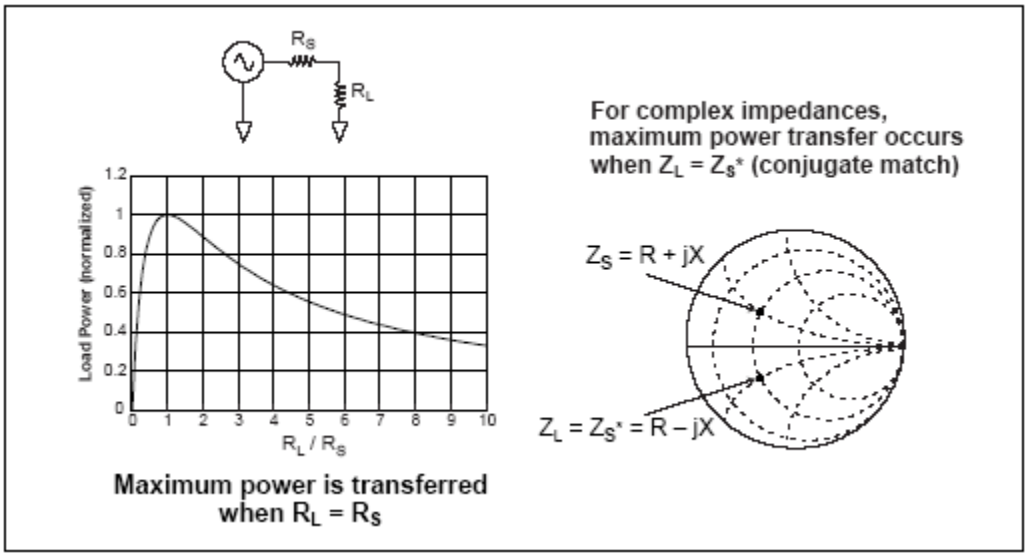

Fig. 2.3 Power Transfer

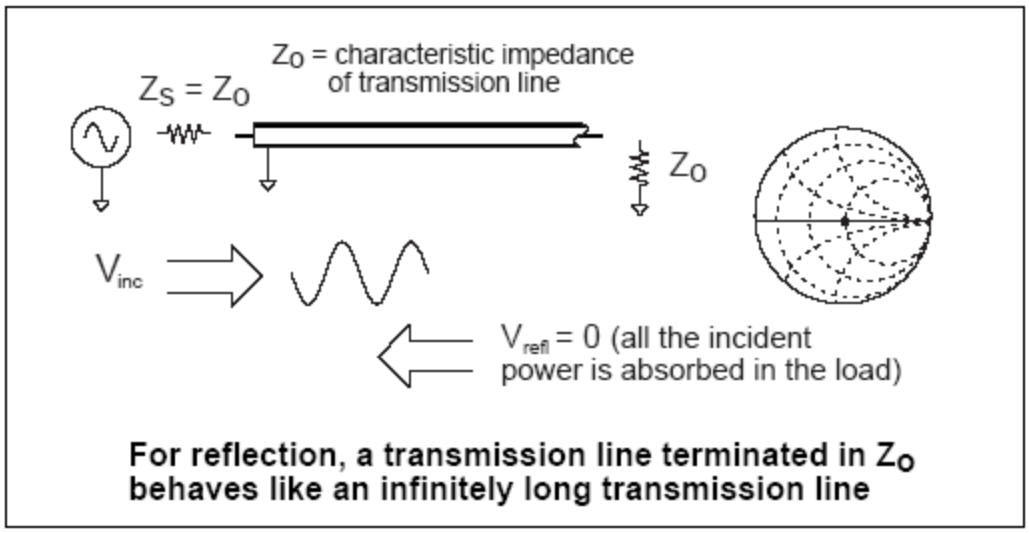

Fig.2.4 Transmission line termination with Z_0

When the transmission line is terminated in a short circuit (which can sustain no voltage and therefore dissipates zero power), a reflected wave is launched back along the line toward the source (Figure 2.5). The reflected voltage wave must be equal in magnitude to the incident voltage wave and be 180 degrees out of phase with it at the plane of the load. The reflected and incident waves are equal in magnitude but traveling in the opposite

directions. If the transmission line is terminated in an open-circuit condition (which can sustain no current), the reflected current wave will be 180 degrees out of phase with the incident current wave, while the reflected voltage wave will be in phase with the incident voltage wave at the plane of the load. This guarantees that the current at the open will be zero. The reflected and incident current waves are equal in magnitude, but traveling in the opposite directions. For both the short and open cases, a standing wave pattern is set up on the transmission line. The voltage valleys will be zero and the voltage peaks will be twice the incident voltage level. If the transmission line is terminated with say a 25-ohm resistor, resulting in a condition between full absorption and full reflection, part of the incident power is absorbed and part is reflected. The amplitude of the reflected voltage wave will be one-third that of the incident wave and the two waves will be 180 degrees out of phase at the plane of the load. The valleys of the standing-wave pattern will no longer be zero, and the peaks will be less than those of the short and open cases. The ratio of the peaks to valleys will be 2:1. The traditional way of determining RF impedance was to measure VSWR using an RF probe/detector, a length of slotted transmission line, and a VSWR meter. As the probe was moved along the transmission line, the relative position and values of the peaks and valleys were noted on the meter. From these measurements, impedance could be derived. The procedure was repeated at different frequencies. Modern network analyzers measure the incident and reflected waves directly during a frequency sweep, and impedance results can be displayed in any number of formats (including VSWR).

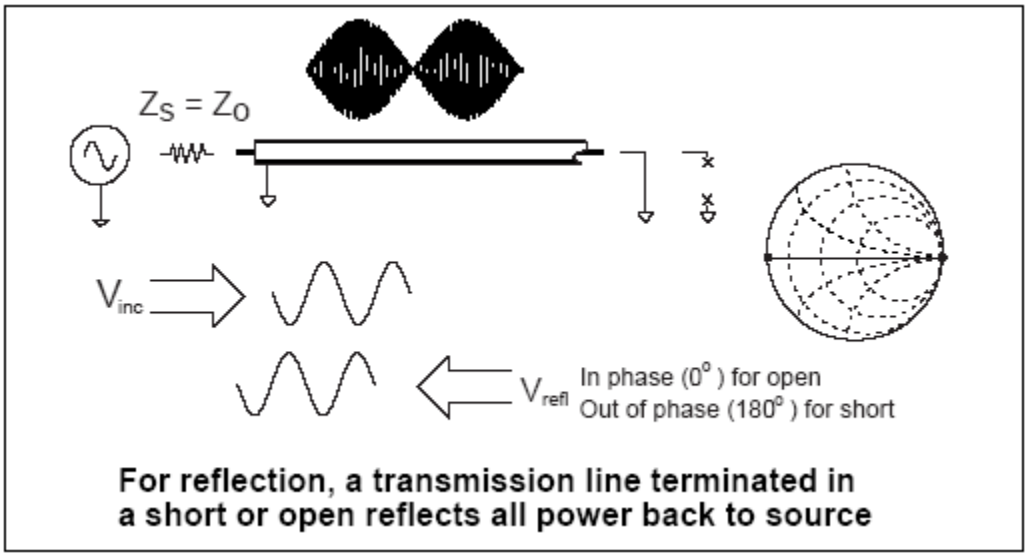

Fig.2.5 Transmission line terminated with short, open

2.4.5 Network Analysis Terminology

Now that we understand the fundamentals of electromagnetic waves, we must learn the common terms used for measuring them. Network analyzer terminology generally denotes measurements of the incident wave with the R or reference channel. The reflected wave is measured with the A channel, and the transmitted wave is measured with the B channel (Figure 2.6). With the amplitude and phase information in these waves, it is possible to quantify the reflection and transmission characteristics of a DUT. The reflection and transmission characteristics can be expressed as vector (magnitude and phase), scalar (magnitude only), or phase-only quantities. For example, return loss is a scalar measurement of reflection, while impedance is a vector reflection measurement.

Rationed measurements allow us to make reflection and transmission measurements that are independent of both absolute power and variations in source power versus frequency. Rationed reflection is often shown as A/R and rationed transmission as B/R, relating to the measurement channels in the instrument.

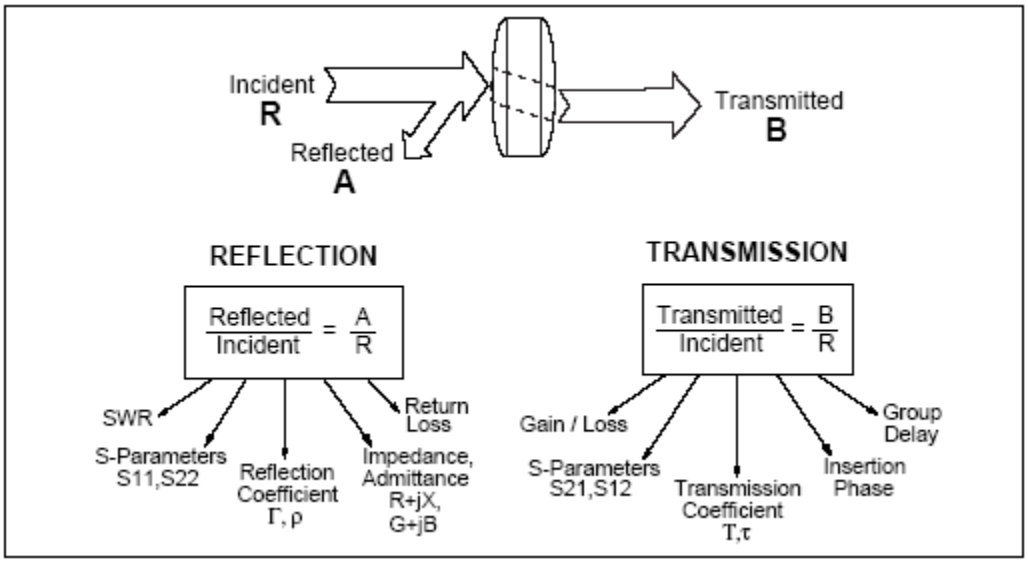

Fig.2.6 Common term for high frequency device characterization

The most general term for ratioed reflection is the complex reflection coefficient, Γ or gamma (Figure 2.7). The magnitude portion of Γ is called ρ or rho. The reflection coefficient is the ratio of the reflected signal voltage level to the incident signal voltage level. For example, a transmission line terminated in its characteristic impedance Z_0, will have all energy transferred to the load so $V_{refl} = 0$ and $\rho = 0$. When the impedance of the load, Z_L is not equal to the characteristic impedance, energy is reflected and r is greater than zero. When the load impedance is equal to a short or open circuit, all energy is reflected and $\rho = 1$. As a result, the range of possible values for ρ is 0 to 1.

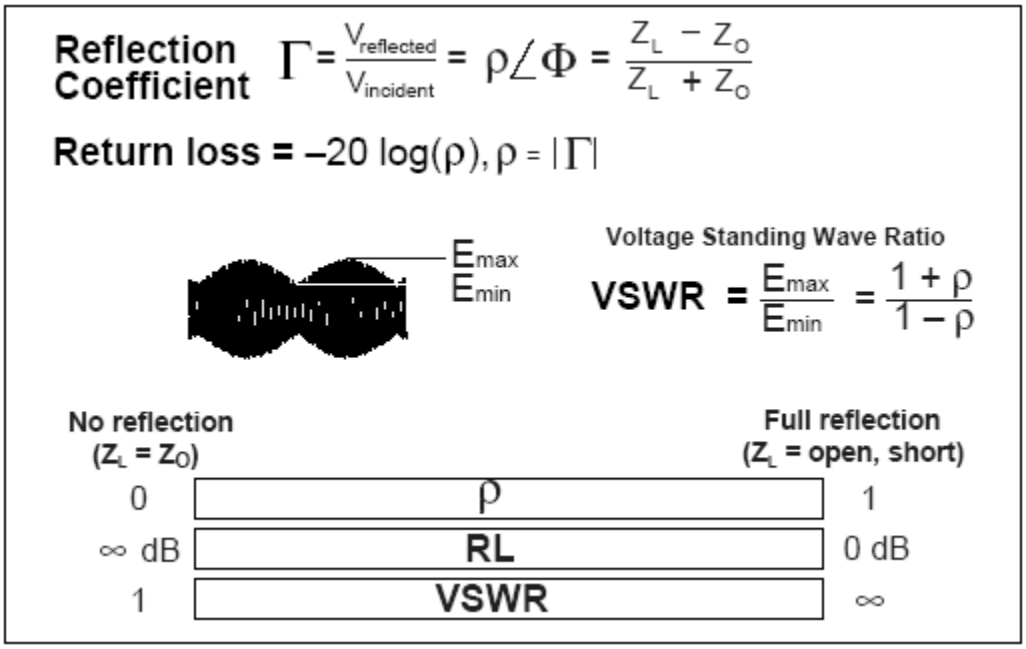

Fig.2.7 Reflection parameters

Return loss is a way to express the reflection coefficient in logarithmic terms (decibels). Return loss is the number of decibels that the reflected signal is below the incident signal. Return loss is always expressed as a positive number and varies between infinity for a load at the characteristic impedance and 0 dB for an open or short circuit. Another common term used to express reflection is voltage standing wave ratio (VSWR), which is defined as the maximum value of the RF envelope over the minimum value of the RF envelope. It is related to ρ as (1 + ρ)/(1 – ρ). VSWR ranges from 1 (no reflection) to infinity (full reflection). The transmission coefficient is defined as the transmitted voltage divided by the incident voltage. If the absolute value of the transmitted voltage is greater than the absolute value of the incident voltage, a DUT or system is said to have gain. If the absolute value of the transmitted voltage is less than the absolute value of the incident voltage, the DUT or system is said to have attenuation or insertion loss. The phase portion of the transmission coefficient is called insertion phase.

2.4.6 Network Characterization

In order to completely characterize an unknown linear two-port device, we must make measurements under various conditions and compute a set of parameters. These

parameters can be used to completely describe the electrical behavior of our device (or network), even under source and load conditions other than when we made our measurements. Low-frequency device or network characterization is usually based on measurement of H, Y, and Z parameters. To do this, the total voltage and current at the input or output ports of a device or nodes of a network must be measured. Furthermore, measurements must be made with open-circuit and short-circuit conditions. Since it is difficult to measure total current or voltage at higher frequencies, S-parameters are generally measured instead (Figure 2.8). These parameters relate to familiar measurements such as gain, loss, and reflection coefficient. They are relatively simple to measure, and do not require connection of undesirable loads to the DUT. The measured S-parameters of multiple devices can be cascaded to predict overall system performance. S-parameters are readily used in both linear and nonlinear CAE circuit simulation tools, and H, Y, and Z parameters can be derived from S-parameters when necessary.

The number of S-parameters for a given device is equal to the square of the number of ports. For example, a two-port device has four S-parameters. The numbering convention for S-parameters is that the first number following the S is the port at which energy emerges, and the second number is the port at which energy enters. So S21 is a measure of power emerging from Port 2 as a result of applying an RF stimulus to Port 1. When the numbers are the same (e.g. S11), a reflection measurement is indicated.

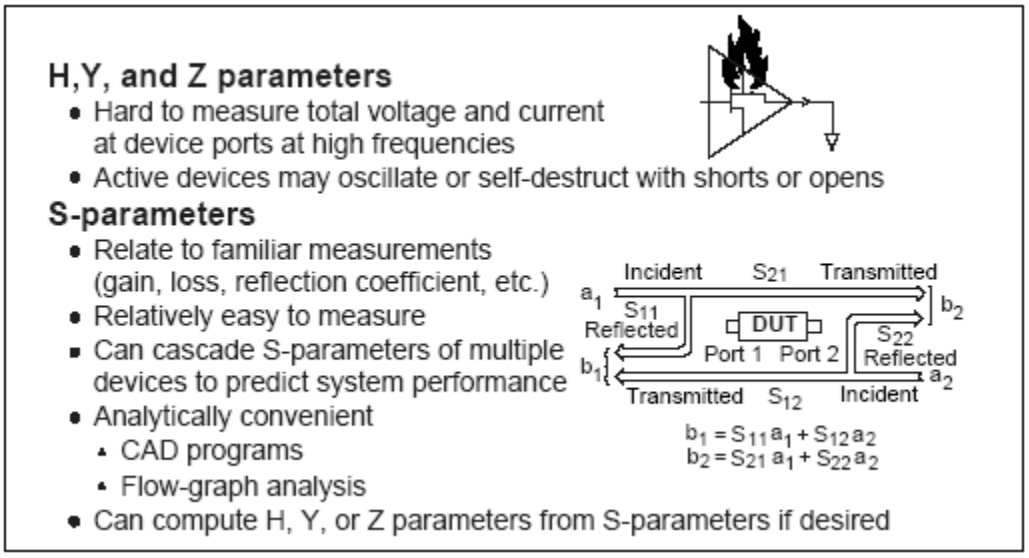

Fig.2.8 Limitations of H, Y, Z parameters

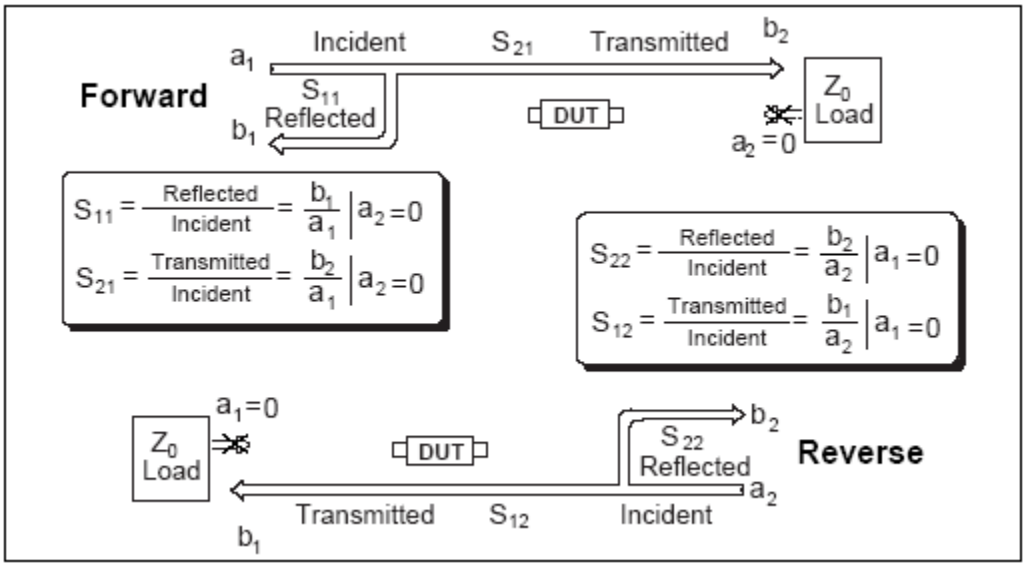

Fig.2.9 Measuring S-parameters

Forward S-parameters are determined by measuring the magnitude and phase of the incident, reflected, and transmitted signals when the output is terminated in a load that is precisely equal to the characteristic impedance of the test system. In the case of a simple two-port network, S11 is equivalent to the input complex reflection coefficient or

impedance of the DUT, while S21 is the forward complex transmission coefficient. By placing the source at the output port of the DUT and terminating the input port in a perfect load, it is possible to measure the other two (reverse) S-parameters. Parameter S22 is equivalent to the output complex reflection coefficient or output impedance of the DUT while S12 is the reverse complex transmission coefficient (Figure 2.9).

2.5 TRANSMISSION MEASUREMENTS OF RESONATOR QUALITY FACTORS USING VECTOR NETWORK ANALYZERS

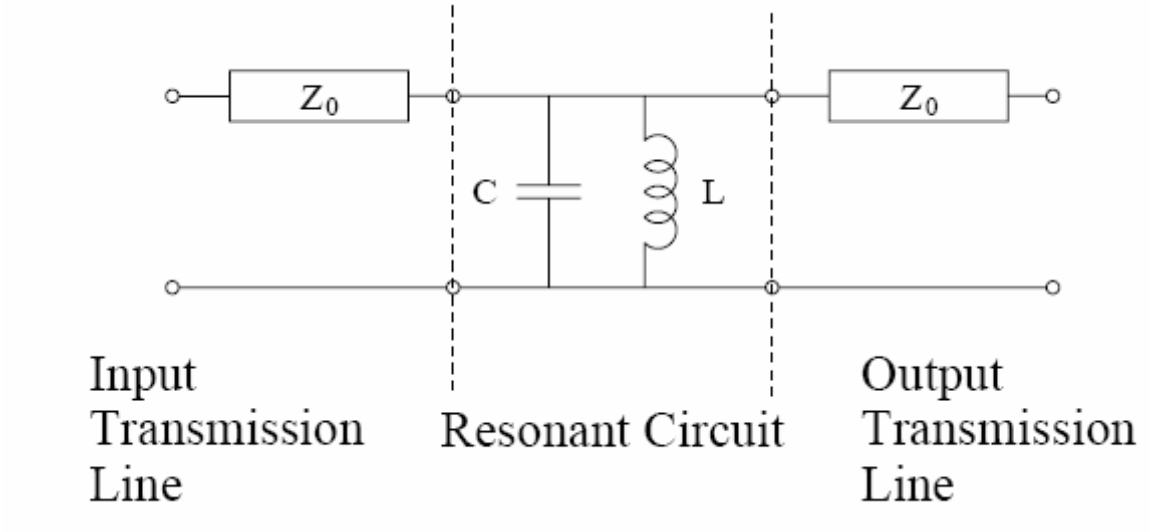

Figure 2.10 A parallel LC circuit

In above Figure 2.10 a parallel *LC* resonant circuit, The *LC* circuit is excited by an incoming wave arriving on the transmission line to the left, and the circuit generates an outgoing wave on the transmission line to the right. For calculating the quality factor of this circuit, the transmission lines can be replaced by resistors, whose resistances are given by the characteristic impedance *Z*0 of the transmission lines. We develop the method by analyzing the simplest possible resonator, namely a parallel *LC* "tank" circuit. The circuit is assumed to be excited by a transmission line of characteristic impedance *Z*0, and the circuit is monitored by a second transmission line with the same characteristic impedance, as shown in Fig. 1. With no excitation, the situation is entirely equivalent to a

parallel *RLC* circuit, where the damping resistance is given by $R = Z0/2$. The quality factor of a parallel *RLC* circuit is given by the well known formula, $Q = \omega 0RC$ (1)

Where $\omega 0 = 1/\sqrt{LC}$ is the resonance frequency. This formula for *Q* agrees with the usual definition, which is the ratio of the average energy stored in the resonator to the power dissipated (lost) per cycle, multiplied by 2π.

2.5.1 Calculation of the scattering matrix

The parallel *LC* circuit may be replaced by an impedance *Z* which is calculated by combining these two elements in parallel. The two–port impedance matrix of a shunt impedance *Z* is given by

$$Z = \begin{bmatrix} z & z \\ z & z \end{bmatrix} \qquad (2.1)$$

And can easily be converted to a scattering matrix normalized to the characteristic impedance Z_0 using

$$S = (z + zI_0)^{-1}(z - zI_0) \qquad (2.2)$$

Where I is the identity matrix. The result is

$$S = \frac{1}{Z_0+2Z}\begin{bmatrix} -Z_0 & 2Z \\ 2Z & -Z_0 \end{bmatrix} \qquad (2.3)$$

In particular, the matrix element for transmission from the input to the output is

$$S_{21} = \frac{2Z}{Z_0+2Z} \qquad (2.4)$$

For the parallel *LC* combination, the total shunt impedance is given by

$$Z = \frac{jwL}{1-w^2LC} \qquad (2.5)$$

2.5.2 The complex S21 plane

It is easy to see, both physically and from equation (6), that the shunt impedance vanishes ($Z \to 0$) as $\omega \to 0$ and $\omega \to \infty$. Thus, in these limits, the shunt impedance short–circuits

the connection between the input and output transmission lines and prevents any signal from being transmitted: $S21 \rightarrow 0$. At resonance, the admittances of the inductance and capacitance cancel so $Z \rightarrow \infty$. In this case, the tank circuit "disappears", and we get perfect transmission, $S21 \rightarrow 1$. The behavior of $S21$ with frequency is shown in Fig. 2. The trajectory is a circle, starting at the origin, sweeping through $S21 = 1$ at resonance, and returning to the origin at high frequencies.

2.5.3 Determining the quality factor

The points B and D, located on the S_{21} trajectory midway between the origin A and resonance peak C (see Fig.2.11, play a special role in determining the quality factor. These points, which

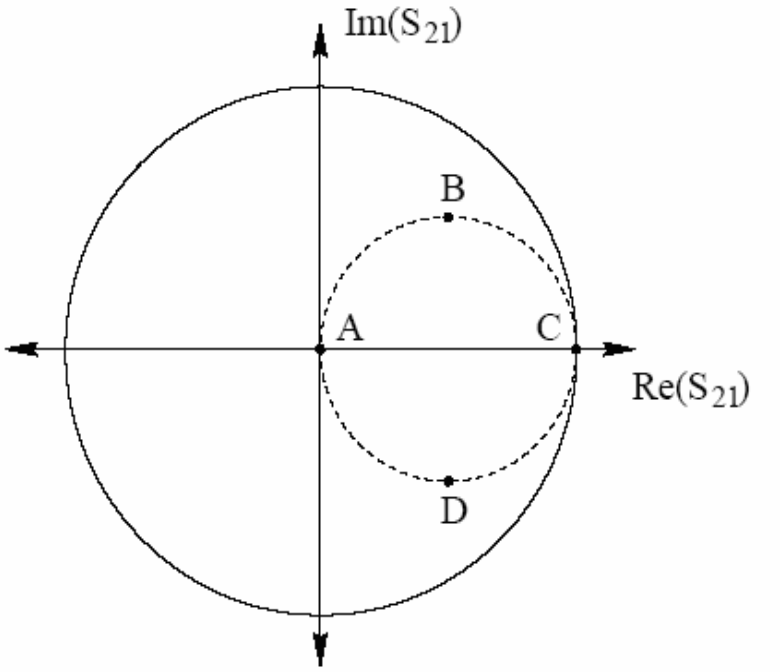

Figure 2.11 Behavior of the complex transmission coefficient S_{21}

The generic behavior of the complex transmission coefficient S_{21} as a function of frequency for an ideal resonant circuit. The transmission vanishes at low frequencies (point A); moves through points B, C, D as the frequency is swept up through the resonance, and returns to point A at high frequencies, are defined by $S21 = (1 \pm j)/2$,

correspond to shunt impedance values of $Z = \pm jZ0/2$. It is easy to show from equation (6) that the frequencies which correspond to these impedance values are

$$w \approx w_0[1 \pm \frac{1}{2Q}] \qquad (2.6)$$

Where Q is given by equation (1), This means that we can calculate Q simply by finding the central frequency of the resonance v_0 from point C, frequency separation Δv_{BD} between points B and D, and dividing to determine Q

$$Q = \frac{\nu_0}{\Delta \nu_{\mathrm{BD}}} \qquad (2.7)$$

2.6 FREQUENCY MEASUREMENT PROCEDURE OF MICROWAVE CAVITY

We use the VNA model wiltron 372xxxB used for measurement the quality factor and resonance frequency of microwave cavity.

Setup of the Vector network analyzer

- Calibrate the network analyzer and the measurement line after connecting an appropriate adapter. Since only S11 measurement will be done, S11 one-port calibration is enough.
- Set measurement as S11.
- Set format to Log-mag.
- Set the frequency range from 6 GHz to 8 GHz.
- Enlarge the frequency range near the resonance peak after you find the resonance.
- Note down the resonance centre frequency by putting the pointer at resonance peak.

2.7 PERTURBATION WITH A METAL OBJECT IN THE CAVITY

The frequency changed due to a metal inside the cavity is described as follows [1].

$$f^2 = {f_0}^2\{1 + \int({H_0}^2 - {E_0}^2)dv\} \qquad (2.8)$$

Where f_0 is the resonant frequency without an object inside the cavity. The second term in the brackets is an integral over the volume removed by the object. If you put a bead on the beam axis in the acceleration gap, frequency becomes lower since there is no magnetic field. In other words, you can measure the relative field strength by measuring the frequency shifts at different locations of the bead. This is so-called a bead-pull method.

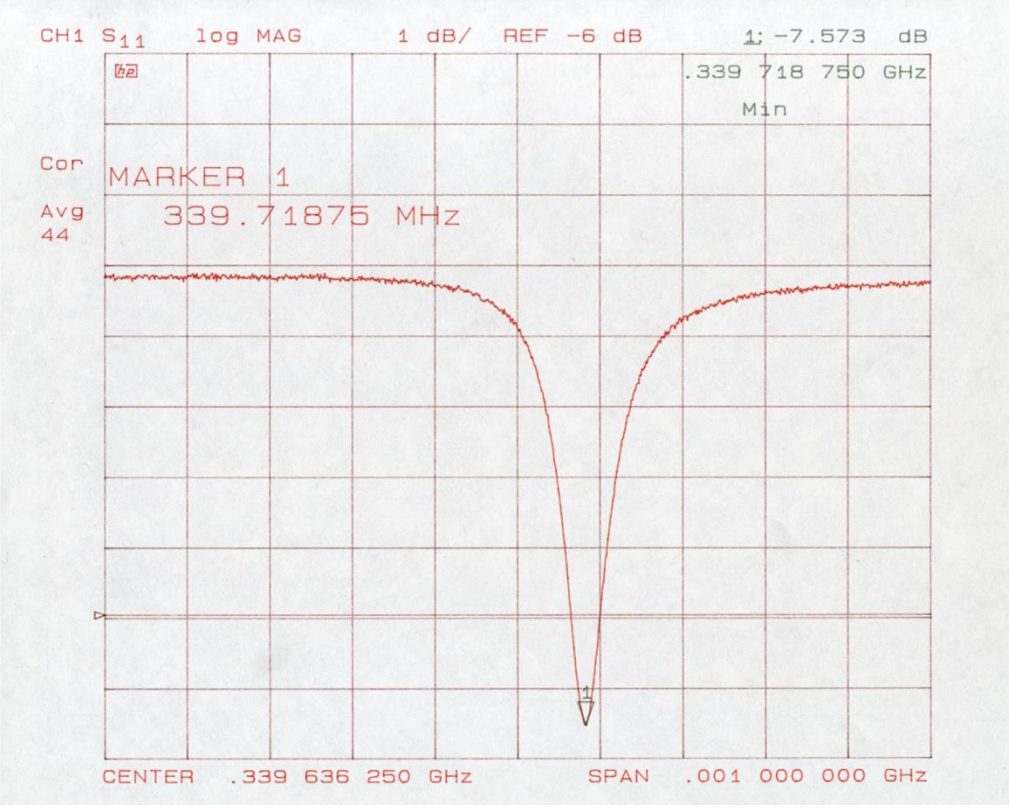

Fig.2.12 A S_{11} plot using loop-type probe inserted through the side port.

CHAPTER 3
MICROWAVE CAVITY

3.1 RESONATOR

In a number of applications, ranging from mobile personal communication through improved Doppler radar for collision avoidance and target identification to improved global satellite navigation systems there is a need for improvement in the performance of frequency selective elements such as filters and resonators.

Resonance is a phenomenon which occurs when two opposite kind of energy storing elements are present in the circuit, for example, likes the inductor and capacitor. The response is said to be resonant if circuit behavior is resistive in nature.

3.2 CAVITY RESONATOR

Any perfectly conducting surface enclosing a finite volume possesses an infinite number of discrete stationary solutions for a standing electromagnetic wave within the volume. For the surface enclosing a volume with high symmetry (sphere, cylindrical, rectangular, parallelepiped etc.) simple analytical solution exist for the electric and magnetic field spatial distributions and the Eigen frequencies of these resonant modes. For the cavity resonator with high symmetry these modes can be classified as transverse electric (TE) or transverse magnetic (TM) modes. If the surface is allowed to possess finite conductivity the eigen frequencies become slightly downwards and also broadened, to reflect the damping of stored electromagnetic energy in the time domain.

3.3 TYPE OF MICROWAVE CAVITY

Mainly the microwave cavities are three types-

- Rectangular Waveguide Cavity
- Circular Waveguide Cavity
- Cylindrical Cavity Resonator

3.3.1 Rectangular Waveguide Cavity

Rectangular Parallelepiped resonators are constructed from close section of waveguides because of radiation losses from open-ended waveguide. Waveguide resonators are usually short circuited at both the ends,thus forming a closed box or cavity. Electric and magnetic energy is stored within the cavity; the power can be dissipated in the metallic walls of the cavity as well as in the dielectric filling within the cavity.

The resonant frequency of the TE_{nml} or TM_{nml} mode is given by

$$f_{nml} = \frac{c}{2\pi\sqrt{\mu_r \epsilon_r}} \sqrt{\left(\frac{n\pi}{a}\right)^2 + \left(\frac{m\pi}{b}\right)^2 + \left(\frac{l\pi}{d}\right)^2} \qquad (3.1)$$

If b<a<d, the dominant resonant mode (lowest resonant frequency) will be the TE_{101} mode. The TM mode is the TM_{110} mode.

3.3.2 Circular Waveguide Cavity

Dominant TE mode is cylindrical cavity is TE111 while the dominant TM mode is TM_{110}. The resonant frequency of TE_{nml} Mode is given by

$$f_{nml} = \frac{c}{2\pi\sqrt{\mu_r \epsilon_r}} \sqrt{\left(\frac{x'_{nm}}{a}\right)^2 + \left(\frac{l\pi}{d}\right)^2} \qquad (3.2)$$

The resonant frequency of TM_{nml} is given by

$$f_{nml} = \frac{c}{2\pi\sqrt{\mu_r \epsilon_r}} \sqrt{\left(\frac{x_{nm}}{a}\right)^2 + \left(\frac{l\pi}{d}\right)^2} \qquad (3.3)$$

3.3.3 Cylindrical Cavity Resonator

A cavity resonator can be considered as volume enclosed by conducting surfaces and within which an electromagnetic field can be excited. Average electric energy We and magnetic energy Wm, stored in the volume of the cavity are given by

$$W_e = \tfrac{1}{4}\varepsilon \int |E|^2 \, dV \qquad (3.4)$$

$$W_m = \tfrac{1}{4}\varepsilon \int |H|^2 \, dV \qquad (3.5)$$

Where |E| and |H| are the complex amplitudes of electric and magnetic fields inside the resonator, V is the volume of the cavity and ε and μ are the permittivity and permeability of the medium enclosed by the cavity walls.

The total energy W_t stored inside the cavity is the sum of the stored electric and magnetic energies i.e.

$$W_t = W_e + W_m$$

Under the condition of resonance, the total stored energy is constant as a function of time. The energy alternates between being stored in the electric and magnetic fields. In the phase approach, the average values of We and Wm arte equal therefore

$$W_t = 2W_e = 2W_m$$

The uploaded Quality factor Q_o, is the figure of merit for assessing the performance or quality of a resonator defined as

$$Q_0 = 2\pi f_0 \frac{w_t}{P_l}$$

Where f_0 is the resonant frequency, W_t is the total energy stored and P_l is the average power loss. In the case of hollow cavity resonator, power dissipates only due to conduction loss that arises as a result of finite conductivity of the cavity walls. The dielectric and radiation loss are negligible compared to the conductive loss, therefore, Qo can be expressed as

$$\frac{1}{Q} = \frac{1}{2\pi f_0 \varepsilon_0} \frac{R_s \int |J_s|^2 ds}{\int |E|^2 dv}$$

R_s is the surface resistance of the material of the walls of the cavity. εo is the permittivity of the medium enclosed by the cavity walls can be deduced from the component of the magnetic field Ħ parallel to the surface of the cavity wall by the relation

$$Js = \hat{} \, n * H$$

Where ^ n is the unit vector normal to the surface of the cavity wall.

Cylindrical cavity resonator although have high Q of 10^4 or more; they are not well suited for integration in miniature microwave integrated circuitry. Another disadvantage of metal cavity is the significant frequency drift caused by the dimensional expansion due to the variation in temperature. The dielectric resonator overcome most of the disadvantages as it can have an unloaded Q as high as several thousands, being compact it is easily integrated with planar circuitry.

3.4 MAIN FEATURES OF THE MICROWAVE CAVITY

The microwave cavity is used essentially for two purposes: providing the microwave field interrogating the 87Rb atom in the cell and using as the band-pass filter for the microwave frequency multiplier and mixer.

To satisfy the requirements of the miniature rubidium frequency standard, the microwave cavity designer should take four factors into account. Firstly, it is necessary to generate the microwave magnetic field parallel to the quantization axis in the microwave resonant region. Secondly, the quality factor of the cavity is appropriately chosen. Thirdly, the resonant frequency of the cavity is close to 6.834 GHz, corresponding to the clock transition between the hyperfine levels (F=1, m_F=0), and (F=2, m_F=0). Last, the cavity size should be as small as possible.

3.5 MODE

There is infinite number of different possible solutions for Maxwell's equation arising from the expression for E_z and each solution was said to give rise to a different mode of propagation in the waveguide.

$$E_z(x, y, z, t) = E_0(x, y, z)e^{jwt}$$

$$H_z(x, y, z, t) = H_0(x, y, z)e^{jwt}$$

Mode further divided of propagation into those modes where E_z exit but $H_z = 0$ are called "Transverse Magnetic"(TM) mode. Similarly where H_z exit and $E_z = 0$ then they

are called “Transverse Electric” (TE) mode. TE and TM modes further divided according to values of m, n integer.

n = for electric field, it is the order of Bessel function and is a measure of circumferential variation in the field.

m = is the number of zero of Bessel function of order ‘n’ and it is a measure of radial variation of the field.

$$\lambda_c = \frac{1}{\sqrt{[\left(\frac{m}{2a}\right)^2 + (\frac{n}{2b})^2]}}$$

Above expression shows that different modes will have different frequencies below which propagation is cut-off and that this cut-off frequency is approximately a function of m, n.

Hence mode with the lowest possible values of m & n will be able to propagate at the lowest frequencies and there will be a band of frequencies over which only this mode will be able to propagate. This is called “Dominant mode”.

For cylindrical cavity TE11 is the dominant mode and for rectangular cavity TE10 is the dominant mode.

3.6 THE CHOICE OF CAVITY MODE

The choice of a proper cavity mode is important in realizing a downsized cavity [14]. The microwave cavity for the RFS is usually operated in three modes: TE_{011}, TE_{111} and TE_{101}. Among the existing cavities, the quality factor of cavity operated in the TE_{011} mode is maximal, and the region where the microwave magnetic field intensity is strongest is just the center of the light-microwave resonance in the integrated cell, so the filling factor is highest. Unfortunately, this mode at the rubidium resonance frequency of 6834MHz requires a minimum diameter of about 70mm, and it is impossible to substantially reduce this size by a dielectric filling. And TE_{011} mode is not the dominant mode of a cylindrical cavity resonator. Therefore, this type of cavity is not suited to the cavity miniaturization. The case of the rectangular cavity operated in mode TE101 is slightly different from other

cavities since a dielectric slab is inserted along one of its sides in order to eliminate the variation of the stimulating field along the X-axis. The dimension of this cavity is minimal among the three mode cavities, but the filling factor is so small, that it is rarely used in the RFS. Considering both the filling factor and the size of the cavity together, we select the cylindrical cavity operated in the mode TE_{111}, which is the dominant mode of a cylindrical cavity resonator.

The magnetic field intensity and modes consider for cylindrical microwave cavity [1] is given by the expression

$$H_z = \frac{k_3}{k} J_l(k_1 r)\cos(l\theta)\sin(k_3 z) \qquad 3.6(a)$$

$$H_r = \frac{k_3}{k} J'_l(k_1 r)\cos(l\theta)\cos(k_3 z) \qquad 3.6(b)$$

$$H_\theta = -l\frac{k_3}{k}\frac{J_l(k_1 r)}{k_1 r}\sin(l\theta)\cos(k_3 z) \qquad 3.6(c)$$

Where cylindrical coordinates are used and the origin is at the centre of the bottom of the cavity. Further more

$$k_1 = \frac{x_{lm}}{D} \quad k_3 = \frac{n\pi}{L} \quad k^2 = {k_1}^2 + {k_3}^2 \quad \lambda = \frac{2\pi}{k}$$

Here x_{lm} is the m^{th} root of $J'_l(x)$. For the TE011 mode x_{lm} =3.832 and for the TE111 mode x_{lm} =1.832 and the D is the diameter and L is the length of cavity. In the TE_{011} mode cavity the resonance cell is generally placed on the axis symmetry and attached to the bottom of the cavity. The optical pumping light beam passes through the middle of the cavity through circular end opening which do not affect the shape of the magnetic lines of force much.

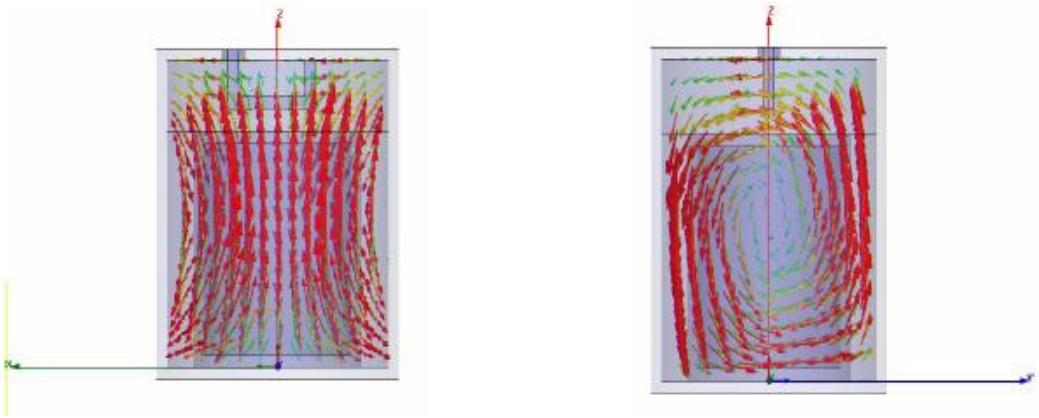

Fig.3.1. Distribution of microwave magnetic field

The RF magnetic field in this mode is predominantly along the Z axis and, with the DC magnetic field orientation [14] as shown in figure 4.1 from the simulation results of microwave magnetic field in the cavity, the arrangement is appropriate for the excitation of $\nabla m_F = 0$ transitions. The radial RF component may excite the $\nabla m_F = \pm 1$ transitions. However, this component is relatively weak in the symmetry consideration. These resonances are weak. Furthermore, at the DC magnetic field intensity normally applied, they are from the central (0,0) transition of interest.

Most of frequency standards presently used TE_{111} cavity because it is much smaller in size than TE_{011} cavity. The resonance cell is allowed to fill the entire space inside the cavity. It observed from that I this mode the z component of the magnetic field is zero in the middle of the cavity. This does not cause problem because, according to equation 3.6(a), the field grows rapidly with radius (R).

In both TE_{011} and TE_{111} modes, the presence of the resonance cell inside the cavity causes a noticeable dielectric loss, with a reduction of the cavity quality factor Q.

The expression for resonance wavelength of cylindrical cavity thus becomes

$$\lambda_{res} = \frac{2}{\sqrt{(\frac{2\chi_{lm}}{\pi D})^2 + (\frac{n}{L})^2}}$$

Both for TE_{lmn} and TM_{lmn} modes, where χ_{lm} is the m[th] root of $J_l(x) = 0$ for the TM waves, and of $J'_l(x) = 0$ for the TE waves. And the resonance frequency

$$(f_{res} D)^2 = (\frac{c\chi_{lm}}{\pi})^2 + \left(\frac{cn}{2}\right)^2 (\frac{D}{L})^2 \qquad (3.7)$$

Where C is the velocity of light.

If we plot $(f_{res} D)^2$ from above equation against $(\frac{D}{L})^2$, we obtained a straight line. This graph is called a mode diagram or mode chart. For any value of D/L, we can read off directly from the graph which mode will be of importance in a limited frequency range.

The point of intersection with the vertical axis is $\left(\frac{c\chi_{lm}}{\pi}\right)^2$

3.7 MODE CHART FOR MICROWAVE CAVITY OF RB ATOMIC CLOCK

Mode chart [18] is useful in determining the shape and size of any cavity so that it will only support one mode over the proposed frequency band of operation.

For our case we choose the TE mode from equation (3.7)

Table 3.1 Resonance frequency vs. dimension ratio

$(D/L)^2$	$(f.D)^2$			
	TE_{111} ($x10^{16}$)	TE_{112} ($x10^{16}$)	TE_{011}($x10^{16}$)	TE_{211}($x10^{16}$)
0	3.0906	3.0906	13.39	8.5051
0.5	4.2156	7.5906	14.51	9.6301
1	5.3406	12.090	15.64	10.755
1.5	6.4656	16.590	16.76	11.880
2	7.5906	21.090	17.89	13.005
2.5	8.7156	25.590	19.01	14.130
3	9.8406	30.090	20.14	15.255
3.5	10.965	34.590	21.26	16.380
4	12.090	39.090	22.39	17.505
4.5	13.215	43.590	23.51	18.630
5	14.340	48.090	24.64	19.755

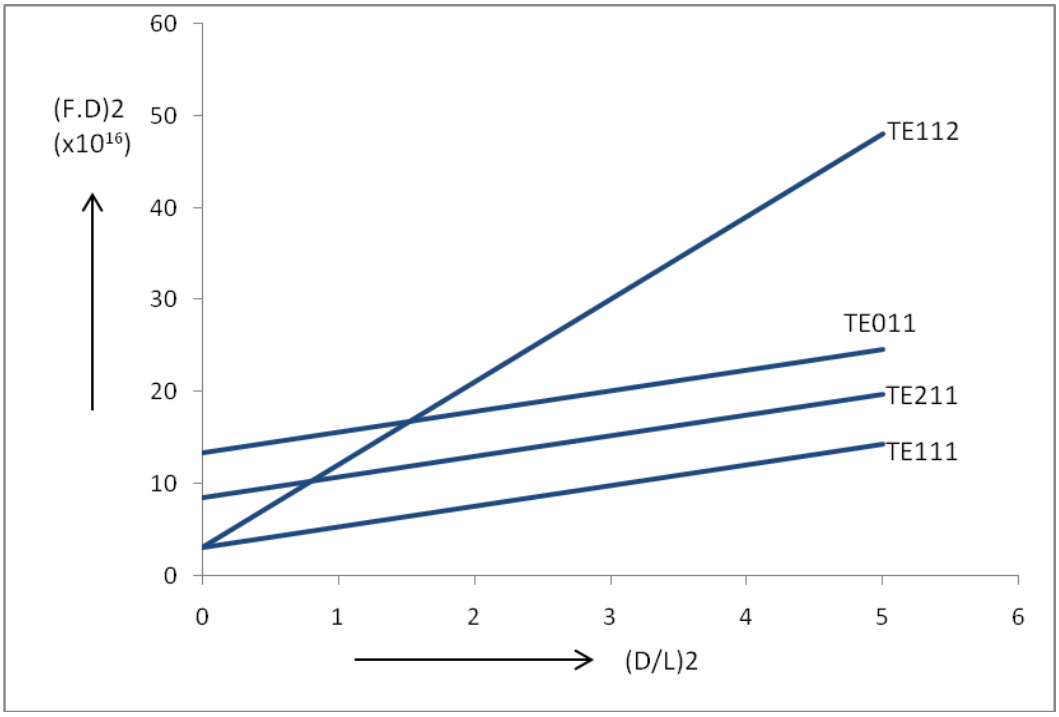

Fig. 3.2 Mode chart on the basis of above table

3.7.1 Importance of circular cavity

- It will be seen that there is a much smaller separation between the cut-off frequency of the dominant mode and of the next mode than in standard rectangular waveguide, so that circular waveguide will operate satisfactorily in a single mode over a much smaller bandwidth than rectangular waveguide.
- Circular cavities are popular since they are easy to make the precise dimensions required.

3.7.2 Cavity material

The cavity must be made with high conductivity material. Cavity can be made of –

- Silver
- High conductive Copper
- Aluminum

3.7.3 Advantage of Aluminum material for cavity

- Al has light weight.
- Al material is space qualified.
- Al is cheaper than other cavity materials.

CHAPTER 4
MAGNETIC SHIELDING

4.1 MAGNETIC SHIELDING

Magnetic interference is caused by low impedance field sources, such as transformers, power supplies, motors etc. In any magnetic shielding problem, there are two choices of components to shield- the source or the components being affected.

Before beginning to solve a magnetic interference problem, the frequency of the ambient field must be determined. The magnetic shielding range (H field) is from DC to approximately 50 kHz. Although there is some overlap, the RFI range (E field) is considered to be above 20 kHz, and the shielding theory, solutions and materials are different in many respects from magnetic shielding.It is essential to know the frequency of interference field because magnetic shielding are manufactured from high permeability, high-nickel-content alloys designed for maximum effective frequency range of the material. Above that frequency RF shields, which are usually manufactured from copper or aluminum are more effective.

4.2 ZERO GAUSS CHAMBER

Zero Gauss chamber provides a work space having an extremely low magnetic field. This is achieved by high attenuation of both D.C. and A.C. magnetic fields. Zero Gauss chamber are fabricated from high permeability CO-NETIC AA alloy (CO-NETIC is a trade name for perfection Mica's high permeability alloy) in a series of two or more concentrically spaced magnetic shields. Each magnetic shield consists of a cylinder with one closed end and a closed-fitting removable cover on the other end. Of all geometric shapes, a cylindrical configuration is one of the most effective for magnetically shielding a finite space. Each shield is magnetically isolated from the adjacent shields by nonmagnetic spacers. The multiplying effect of successive shields provides substantially greater attenuation of magnetic fields than a magnetic shield of equivalent wall thickness.

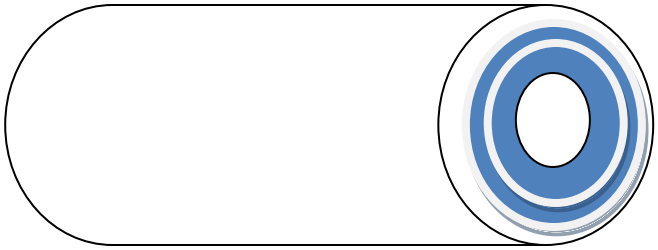

Figure 4.1 Zero gauss chamber

4.3 DESIGN CONSIDERATIONS

4.3.1 Interior Size

For the best result, the inside chamber diameter should be as small as possible because attenuation is inversely proportional to diameter.

$$Attenuation(A) = \frac{permeability \times t}{D}$$

Where D is diameter of the shield in inches and t is thickness of the shield in inches.

Hence, a small shield is desirable because it provides greater attenuation for a given thickness. Additionally the small size is more economical since less material required.

For practical reasons, minimum inside diameter for a double wall chamber is 4 inches (101.6mm) and for triple wall chamber the inside diameter is 6 inches (152.4mm).

4.3.2 External Field Strength

Most Zero Gauss chambers are operated in earth's field, which is usually about 0.5 Gauss. In most environments, there are additional source of magnetic fields, usually 50 Hz and its harmonics. Since all magnetic fields around the chamber are part of the ambient magnetic field, their magnitude must be considered as a part of the shielding requirements. If any of these sources are unusually strong and closed to your apparatus, additional shielding may be required to prevent it.

4.3.3 Attenuation

The number of concentric shields required is a function of the degree of attenuation desired. The external field strength and the maximum allowable magnetic field inside the chamber, or the required attenuation, are decided by the application for which shielding going to be designed.

4.3.4 Wall Thickness

CO_NETIC AA alloy in relatively soft so that the chambers must be fabricated with sufficient wall thickness to maintain the physical integrity of the assembly. The chamber must be support itself and provide sufficient strength to support the item being shielded. Therefore minimum wall thickness is 0.025 inches (0.635 mm).

4.3.5 Access Holes

Holes are provided in the chamber for power and signal cables, degaussing coil leads and other items requiring access to the interior. For best results, holes should be as few and as small possible, with their axes positioned perpendicular (transverse) to the ambient field. The minimum material distance between any two holes in a shield should be equal to the diameter of the larger hole. For construction and alignment purposes, preferred Hole locations are in the closed end or in the removable covers.

Holes in a magnetic shield will allow the interfering field to fringe into the chamber, the amount of leakage is a function of the hole size and the angle between the axis of the hole and the direction of the interference field. Items inside the chamber should be located away from holes. If this cannot be done, then leakage can be substantially reduced with cylindrical shield extensions welded or fastened onto the outer surface of the chamber assembly around the holes.

4.3.6 Spacers

Each CO-NETIC shield of Zero Gauss chamber is magnetically isolated from adjacent shields. Spacing is accomplished longitudinal ½ inch round aluminum spacers 120^{o} apart.

4.3.7 Operating Environment

The final consideration is the operating environment of the Zero Gauss chamber. Normal room conditions usually do not present any problems. High or low operating temperatures may restrict the use of plastics in the handles on the covers and the insulation in the degaussing coil. The operating range of CO-NETIC AA alloy is -269^{o}c to 454 ^{o}c. Operation in vacuum will prevent use of plastics and many finishes because of outgassing.

4.4 MAGNETIC SHIELDING FACTOR FOR RB ATOMIC CLOCK PHYSICS PACKAGE USED THREE CYLINDERS OF HIGH-PERMEABILITY MAGNETIC MATERIAL

In atomic frequency standards, the magnetic shield is composed of several interleaved boxes made of soft material. Generally, they have a shape close to a cylinder with end caps. The thickness is small compared with the other dimensions. The mathematics results enable us the calculation of the efficiency of these shields [16].

The shielding factor of a magnetic shield is define as

$$S = \frac{\text{Increment in external field}}{\text{Increment in internal field}} \qquad (4.1)$$

For a single cylindrical shield with end caps the shielding factor is given by

$$S_t = \frac{1}{2}\,\mu t' \qquad (4.2a)$$

$$S_l = 2D\mu t'(1 + R/L)^{-1} \qquad (4.2b)$$

Where the subscript t stands for transverse and the subscript l for longitudinal. In these expression t' <<1 is the ratio of the material thickness t to the shield radius R, i.e. ($t' = t/R$), L is the length of the shield and D is called the demagnetization factor. It is the function of the L/R. the factor μ is the permeability of the magnetic material. The

permeability μ is approximately 30,000 for molypermalloy and for both longitudinal and transverse fields.

For two such shields with end cap we have

$$S_t = S_{t1}S_{t2}d' + S_{t1} + S_{t2} \quad (4.3a)$$

$$S_l = 2S_{l1}S_{l\,2}fd' + S_{l\,1} + S_{l\,2} \quad (4.3b)$$

Where f is a geometrical factor nearly constant at $f = 0.75$ for 2<L/R<6 and equal to about 0.9 for L/R =10, for instance. d' is given by

$$d' = \frac{1}{2}[1 - (\frac{R_1}{R_2})^2] \quad (4.4)$$

Or, for closely spaced shields,

$$d' \approx \Delta R/R_m \quad (4.5)$$

ΔR being the difference of the shield radius and R_m the average radius of the two shields.

The transverse shielding factor of a system having more than two concentric cylinders with end cap is given by

$$S_t = \frac{1}{2}(\mu_1\mu_2\mu_3 \ldots)(t'_1 t'_2 t'_3 \ldots)(d'_{12}d'_{23}d'_{13} \ldots) \quad (4.6)$$

Where the subscript i characterizes the ith shield and $d'_{i,i+1}$ represents the separation between shields i and $i+1$.

In our case the thickness of cylinder walls are $t_1 = 1.2\ mm, t_2 = 0.7\ mm, t_3 = 0.7\ mm$ thus Transverse Shielding factor for three Cylinders is

$$S_t = \frac{1}{2}\mu^3(t'_1 * t'_2 * t'_3)(d'_{12} * d'_{23} * d'_{13}) \quad (4.7)$$

Where $d'_{12} = \frac{1}{2}[1 - \left(\frac{R_2}{R_1}\right)^2]$, $d'_{23} = \frac{1}{2}[1 - \left(\frac{R_3}{R_2}\right)^2]$, $d'_{13} = \frac{1}{2}[1 - \left(\frac{R_3}{R_1}\right)^2]$.

No general formula for the longitudinal shielding factor of a set of more than two cylindrical shields is available. However, for more than two cylinders an approximate expression for S_l may be obtained by replacing the quantity μ_i by $4D_i\mu_i/(1 + R_i/L_i)$ and the quantity $d'_{i,i+1}$ by $f_i d'_{i,i+1}$ respectively in above equation of S_t, where D_i is magnetization factor of shield cylinder i,

In our case we have, the Longitudinal Shielding factor for three closed cap Cylinders is

$$S_l = \frac{1}{2}[\left(\frac{4D_1\mu 1}{1+\left(\frac{R_1}{L_1}\right)}\right)\left(\frac{4D_2\mu 2}{1+\left(\frac{R_2}{L_2}\right)}\right)\left(\frac{4D_3\mu 3}{1+\left(\frac{R_3}{L_3}\right)}\right)\left(t'_1 t'_2 t'_3\right)\left(d'_{12} d'_{23} d'_{13}\right)\left(f_1 f_2 f_3\right)].$$

…(4.8)

Since in our case $D_1 = D_2 = D_3 = D$ and $f_1 = f_2 = f_3 = f = 0.75$ as 2<L/R<6

Or $$S_l = \frac{64 S_t D^3 f^3}{\{1+\left(\frac{R_1}{L_1}\right)\}\{1+\left(\frac{R_2}{L_2}\right)\}\{1+\left(\frac{R_3}{L_3}\right)\}} \quad (4.9)$$

Now the value of Demagnetization factor is depend on the ratio L/R [2].

$$D = \frac{(1+R/L)}{2*f(1+L/R)} \quad (4.10)$$

Where f is a geometrical factor nearly constant at $f = 0.75$ for 2<L/R<6 and equal to about 0.9 for L/R =10.

For the different value of L/R, the demagnetization factor values , Longitudinal and Transverse shielding factor for our cavity and generalize graphs as well as the variation in shielding factor with permeability discuss in chapter 5.

CHAPTER 5
RESULTS AND DISCUSSION

5.1 MECHANICAL DESIGNING MODIFICATION IN MICROWAVE CAVITY

Initially we design a microwave cavity on the basis of theoretically calculated dimensions through mode chart. This is shown in appendix 1. The inner diameter is 27 mm and the effective length of the cavity is 40 mm. The length is variable for exciting the appropriate mode through the threaded tunable plunger with 10 mm tunable range.

The Resonance frequency and Q factor microwave cavity is measured through the Vector Network Analyzer (Wiltron 37201B model). The result obtained is shown in table 5.1 below.

Table 5.1 Experimental Result for Resonance frequency

Observations	Resonant Freq f_0 (GHz)	Absorption cell	With Photo-detector	f_1 (GHz)	f_2 (GHz)	Δf (GHz)	$Q = f_0/\Delta f$
Set-1	7.8725	No	No	7.8716	7.8734	0.00179	4388.23
	7.5425	Yes	No	7.5396	7.5511	0.01152	654.73
Set-2	7.14497	No	Yes	7.1403	7.14896	0.00866	825.054
	6.8675	Yes	Yes	6.835	6.9011	0.0661	103.89

The above results show that for requiring the resonance frequency 6.834 GHz we need modification in cavity dimension. From the mode chart shown in chapter 3, for the TE111 dominant mode we increase the diameter of cavity by 3 mm and the effective length by 3 mm. Shown in appendix 1.

The second modified version of cavity design matched with our requirements and also provides the tuning frequency without cell and photo-detector from 7.2424 GHz to 8 GHz and with cell from 6.7325 GHz to 7.825 GHz.

5.2 CALCULATION OF RESONANCE FREQUENCY IN TE111 MODE FOR OUR MICROWAVE CAVITY

In our case the cavity length of cavity (L) = 40 mm (variable) which can varies up to 10 mm through threaded plunger and the diameter of cavity (d) = 30 mm (fixed).

By solving the equation (3.7) for TE_{111} we obtained

$$f_{res} = \sqrt{\frac{3.0906\times10^{16}+2.25\times10^{16}(\frac{d}{L})^2}{d^2}} \qquad (5.1)$$

From the above equation (5.1) for different value of L in the step of 2 mm we obtained the theoretical values of unloaded cavity resonance frequency shown in table 5.2.

Table 5.2 Length vs. Resonance frequency

Diameter (d) = 30 mm (fixed)

L (mm)	f_{res} (GHz)
30	7.7032
32	7.5041
34	7.3348
36	7.1901
38	7.0652
40	6.9571

In the above table 5.2 the tuning frequency without cell and detector is approximately from 6.95 GHz to 7.7 GHz.

From table 5.1 the microwave cavity quality factor (Q) decreased with photo-detector which put inside the cavity for sensing the microwave signal. The microwave cavity Q further decreased with absorption cell (without photo-detector) put inside the cavity. When both (photo-detector and absorption cell) put inside the cavity we get the drastically reduction in the microwave cavity Q. Hence the microwave cavity shows the loading effect. Further the results from table 5.2 and microwave cavity developed (with modified design version-2) shows that our designed microwave cavity tuning range is matched with theoretically tuning range for same dimensions.

For the different value of length to radius (L/R) ratio, the demagnetization (D) factor (from equation 4.10) values shown below in table 5.3.

Table 5.3 Demagnetization factor with Dimension Ratio

L/R	Demagnetization factor (D)
2	0.334
3	0.223
4	0.1667
5	0.1334
6	0.112

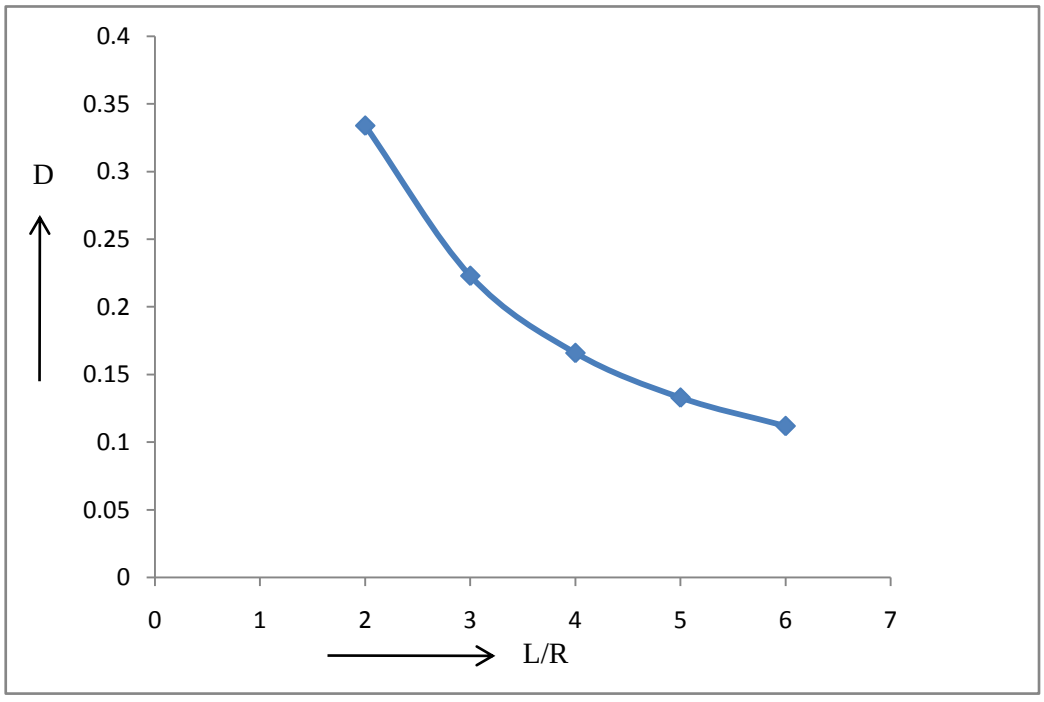

Figure 5.3 Plot variation in D vs L/R

The figure 5.3 shows that the dimension ratio (L/R) must be taken between 2 to 6 for development of cylindrical shielding. Out of this range, experimental value of shielding factor will drastically mismatch with calculated value of shielding factor.

Now for the our case Rb physics package where cylinders lengths are L_1= 200 mm, L_2= 190 mm, L_3= 180 mm and Radius are R_1= 65 mm, R_2= 55 mm, R_3= 45 mm

The Length $L = \frac{L_1+L_2+L_3}{3} =$ 190 mm and Radius R = $\frac{R_1+R_1+R_1}{3} =$55 mm so that the demagnetization factor (from equation 4.10) is **D = 0.19323.**

Now for the above dimensions Transverse and Longitudinal shielding factors (from equations 4.7 & 4.9) are

$$\mathbf{S_t = 301548.84}$$

$$\mathbf{S_l = 27375.85}$$

For generalizing the shielding factor for any value of length in equation (4.9) we varied the length L =200 mm by x i.e. L = 200-x, where x is length variation in mm. Thus we obtained the variation in only Longitudinal shielding factor shown below in table 5.4.

Table 5.4 Longitudinal shielding factor with length variation

$x(mm)$	Longitudinal sh. Factor (S_l)
0	28274.58
10	27336.63
20	26342.64
30	25288.1
40	24168.15
50	22977.62
60	21711.12
70	20363.1
80	18928.15
90	17401.34

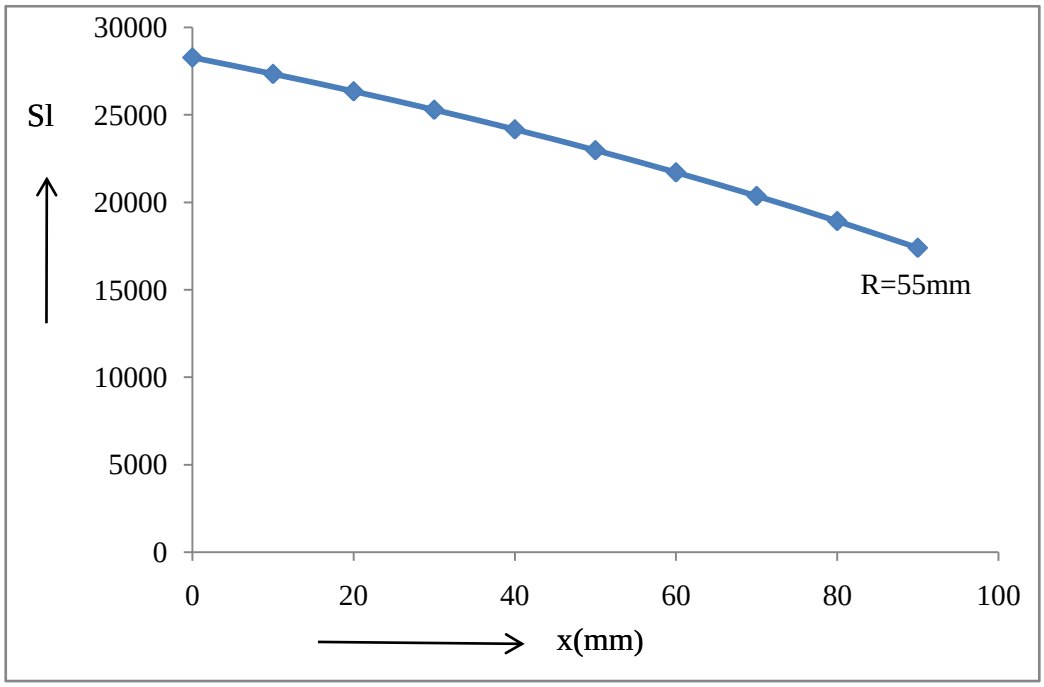

Fig. 5.4 Plot Variation in Length Vs S_l

For different values of radius we also obtained the variation in the Longitudinal as well as Transverse shielding factor for different values of radius. In equation (4.7) and (4.9) we varies the R from 65 mm to descending order up to 35mm and varies it as

$$R_1=65-y, \quad R_2=R1-5, \quad R_3=R_1-10$$

Where y is the radial variation in mm. Thus we obtained the variation in both Longitudinal and Transverse shielding factor shown below in table 5.5.

Table 5.5 Longitudinal & Transverse shielding factor with Radial variation

y(mm)	S_t	S_l
0	31043	3434
5	50936	4612
10	87405	6325
15	158270	8894
20	306070	12886
25	642700	19363
30	1500875	30462

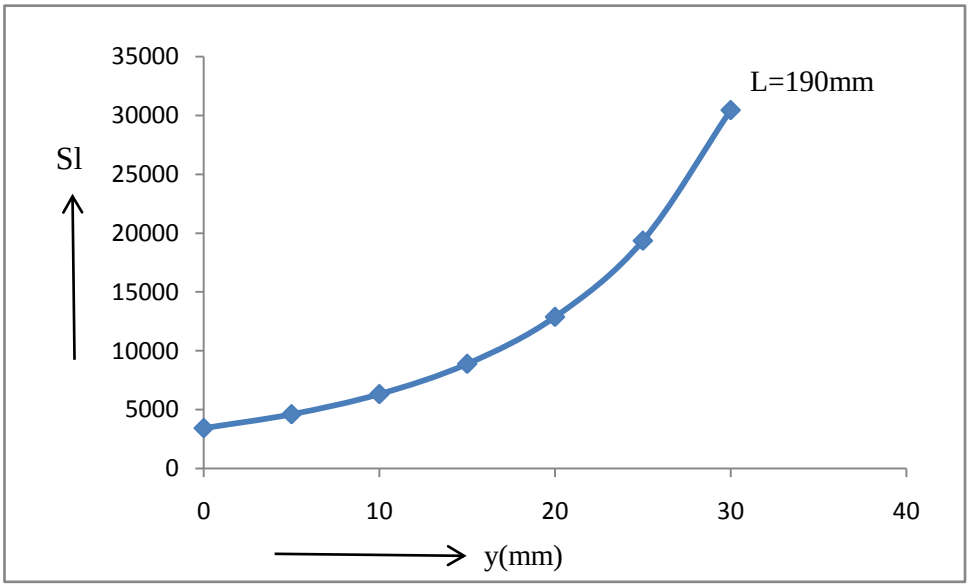

Fig.5.5 Plot radial variation Vs S_l

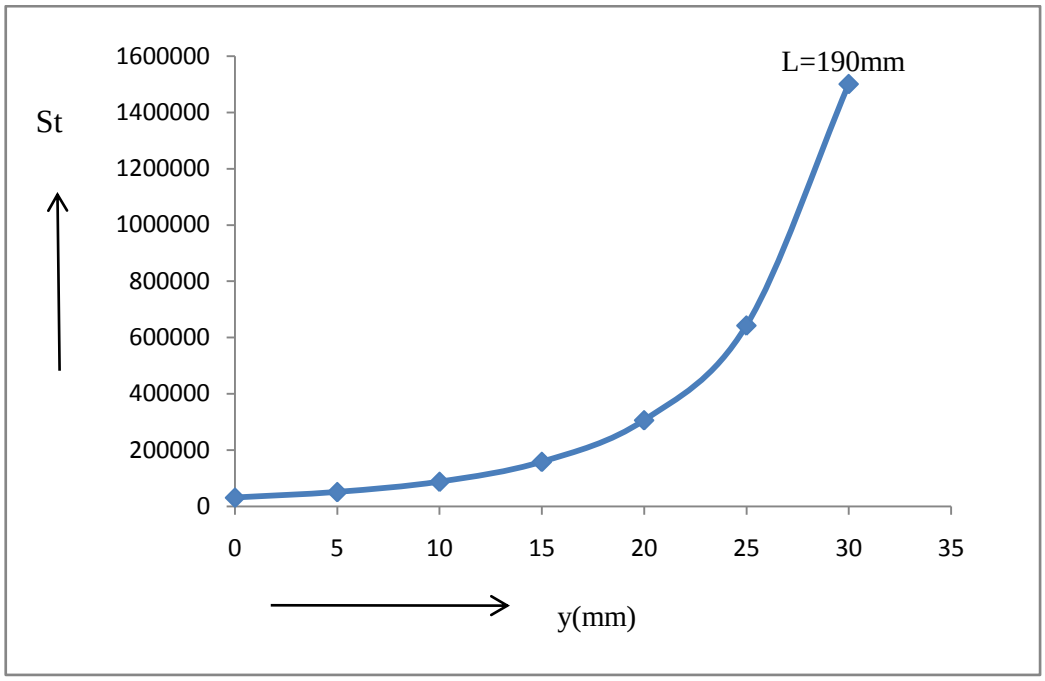

Fig.5.6 Plot radial variation vs. S_t

Hence the above graphs (figure 5.5 & figure 5.7) shows that how the longitudinal and transverse shielding factor increased with increase in radius of shielding cylinder at fixed value of length.

Now for small separation between shielding cylinders let consider

$$R_1 = R_2 = R_3 = R$$

$$L_1 = L_2 = L_3 = L$$

Where R and L are the average radius and average length of the cylinders respectively. Then

$$S_l = \frac{64\, S_t\, f^3 [\frac{1+R/L}{2*f(1+L/R)}]^3}{(1+R/L)^3} \qquad (5.2)$$

Or $$S_l = \frac{8\, S_t}{(1+L/R)^3} \qquad (5.3)$$

We also obtained the variation of longitudinal shielding factor with L/R ratio for 2<L/R<6 at value of $S_t = 301548.84$ shown below in table 5.6.

Table 5.6 Longitudinal shielding factor with Dimension Ratio

L/R	S_l
2	89347.8
3	37693.6
4	19299.1
5	11169.4
6	7033.2

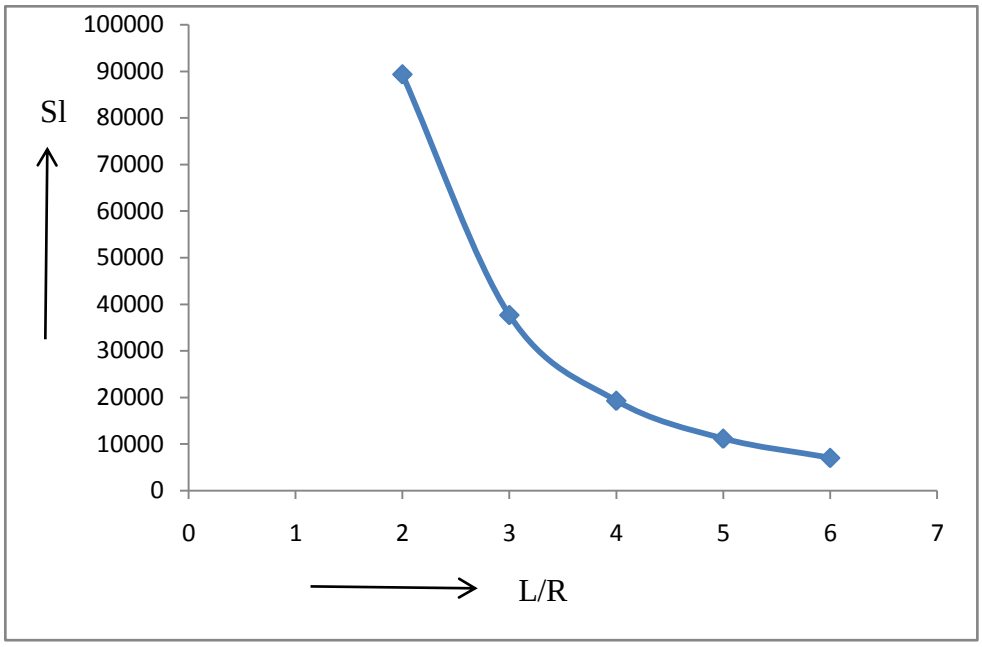

Fig.5.7 Plot S_l vs L/R

The above graph (fig. 5.7) shows the effect of dimensional ratio (L/R) on longitudinal shielding factor. The longitudinal shielding factor exponentially decreased with increase in dimensions ration (L/R).

Further from equation (4.9) we obtained variation in longitudinal shielding factor with permeability for different L/R ratio

Table 5.7 Longitudinal shielding factor with Permeability

μ	**S_I**				
	L/R=2	**L/R=3**	**L/R=4**	**L/R=5**	**L/R=6**
10000	3309	1396	715	413	260
15000	11167.8	4711	2412	1396	879
20000	26472	11168	5718	3309	2084
25000	51703	21812	11168	6463	4070
30000	89343	37692	19299	11168	7033
35000	141873	59853	30647	17735	11168
40000	211776	89344	45747	26473	16672

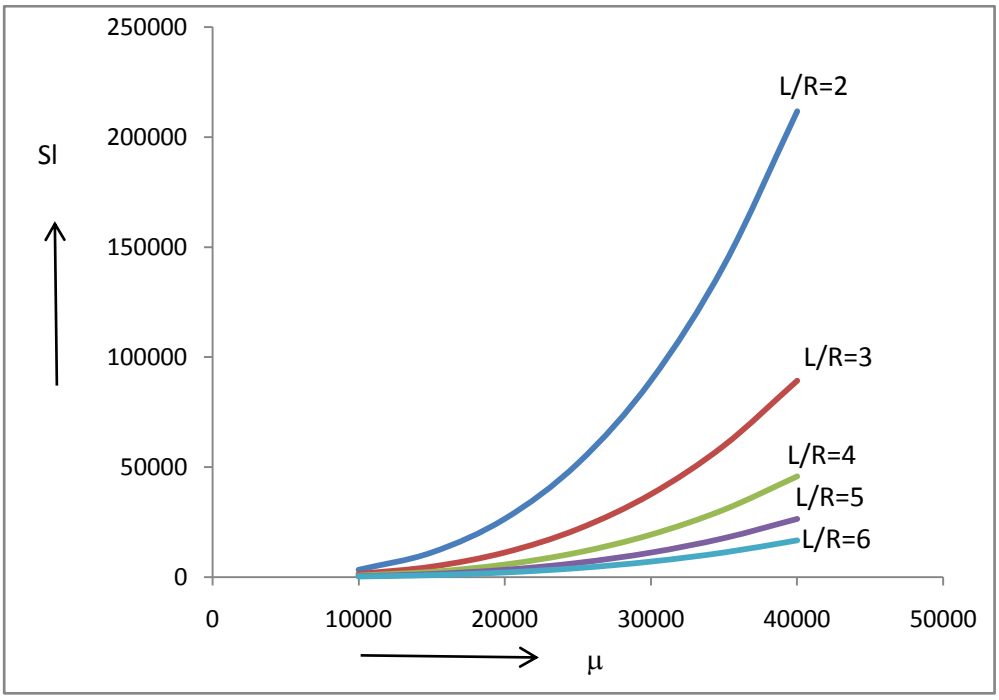

Fig. 5.8 Plot S_I vs. Permeability (μ)

Since magnetic shielding effectiveness required high permeability material to nullify the earth magnetic field fluctuations. This above graph (figure 5.8) shows that magnetic shielding factor increased with increase in permeability. In our case we select the co-netic alloy with high permeability (approximately 30000).

Flowchart to calculate the Transverse and Longitudinal shielding factor For Rb Atomic Clock Physics Package Cylinders

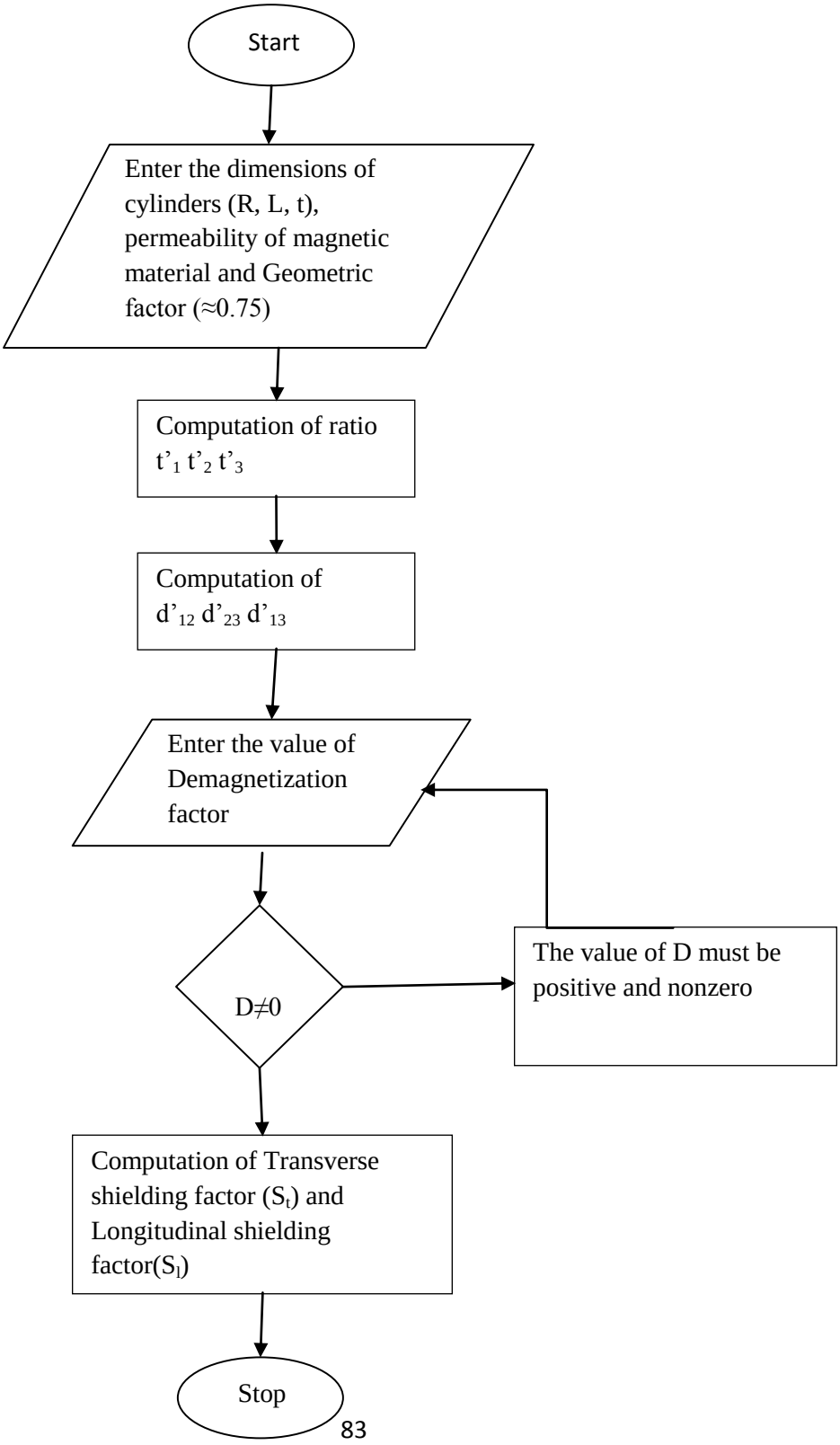

CHAPTER 6

CONCLUSION & FUTURE SCOPE

In this thesis work we have discussed the development and analysis of microwave cavity and magnetic shielding for Rubidium frequency standard. We get the final shape of microwave cavity after the development and analysis of five cavities.

Results show that the Q factor drastically change with loading inside the microwave cavity so that the proper arrangement of absorption cell and the position of photo-detector with appropriate adhesive should be required. The mechanical scratches and grease also affect the Q of microwave cavity so that the microwave cavity must be well finishing and cleaned with chemical solution before testing.

In the second part of thesis we have discussed the longitudinal and transverse Shielding factors of three concentric cylindrical layers of high permeability metal. We have reported calculations for general cases. However, the results reported in thesis are useul in designing magnetic shields for atomic clocks particularly Rb atomic clocks.

The magnetic field pattern can be analyzed by high frequency simulation tool which can provide the more accurate information about the dominant mode as well as couple losses.

Hence as a result the microwave cavity of accurate dimensions can be designed easily and fast.

REFERENCES

[1] Marek Jaworski and Marian W. Pospiezalski "An Accurate Solution of the Cylindrical Dielectric Resonator problem" IEEE TRANSACTION ON MICROWAVE THEORY AND TECHNIQUES , VOL. MMT-27,NO.7, PP.639-643, 1979.

[2] Prof. M.S. Leong , Prof. P.S.Kooi and T.S. Yeo "Tunable Double-ended Dielectric-loaded Microwave Resonator for Frequency Stabilization Applications" IEEE PROC. , VOL.128, Pt. H, NO.4, PP.213-217, 1981.

[3] William J.Riley "A Rubidium Clock For GPS" EG&G, INC., FREQUENCY AND TIME DEPARTMENT, FLIGHT CENTER PROC. OF THE 13th ANNUAL PRECISE TIME, PP.609-630, 1981.

[4] H.E.Williams, T.M.Kwon and T,Moclelland "Compact Rectangular Cavity for Rubidium Vapor-cell Frequency Standard" IEEE 37th ANNUAL SYMPOSIUM ON FREQUENCY CONTROL, PP.12-17, 1983.

[5] Pierre Tremlay, Normand Cyr and Michel Tetu "Evolution Of The Performance Of Passive Rb Frequency Standards Using Cavity Operated In Mode TE011, TE111 And TE101" IEEE 38th ANNUAL FREQUENCY CONTROL SYMPOSIUM, PP.408-415, 1984.

[6] Jovan Lebaric and Darko Kajfez "Mode Evolution for Rotational Symmetry Resonant Cavities Loaded with Inhomogeneous Dielectric" SOUTHEASTCON 88 CONFERENCE PROCEEDINGS IEEE, PP.561-565, 1988.

[7] M.Mohammad Taheri and D.Mirshekar-syahkal "Accurate Determination of Modes in Dielectric Loaded Cylindrical Cavities Using a One Dimensional Finite Element

Method", IEEE TRANCACTION ON MICROWAVE THEORY AND TECHNIQUES , VOL.37, NO.10, PP.1536-1541, 1989.

[8] E.Eltsufin, A.Stern and S.Fel "Compact Rectangular Cylindrical Cavity for Rubidium Frequency Standard" IEEE FORTY- FIFTH ANNUAL SYMPOSIUM ON FREQUENCY CONTROL, PP.11-19, 1991.

[9] Lindon L.Lewis "An Introduction to Frequency Standards" PROCEEDING OF THE IEEE VOL.79, NO.7, PP. 218-223, 1991.

[10] D.watts. F.Li, F.Vu, W.Cashin and T.English "Specifying Commercial Frequency Standards Using Statistics" IEEE INTERNATIONAL FREQUENCY CONTROL SYMPOSIUM, PP.1023-1031, 1996.

[11] Hosokawa Mizuhik "Basic Physics in The Atomic Frequency Standards" JOURNAL OF THE NATIONAL INSTITUTE OF THE INFORMATION AND COMMUNICATION TECHNIQUE, VOL.50, PP.27-38, 2003.

[12] C.Audoin "Understanding How the Smart Rubidium Technology" JOURNAL OF SPECTRA TIME, PP.1-5, 2003.

[13] Andreas Bauch "Cesium Atomic clock Functions Perforation and Application" JOURNAL OF INSTITUTE OF PHYSICS MEASUREMENT SCIENCE AND TECHNOLOGY 14 PP. 1159-1173, 2003.

[14] Yan Wang, Fang Yu, Zhiyong Cheng, Daobang Lu, Chao Li, Xin Jin, WeiGao, KelinGao and Rongwu Sheng "A Downsized Microwave Cavity for the Rubidium Vapor Cell Frequency Standard" FREQUENCY CONTROL SYMPOSIUM, JOINT WITH THE 21st EUROPEAN FREQUENCY AND TIME FORUM. IEEE INTERNATIONAL, PP. 595-598, 2007.

[15] James Camparo, “The Rubidium Atomic Clock and Basic Research” PHYSICS TODAY, AMERICAN INSTITUTE OF PHYSICS VOL. 3, PP. 33-37, 2007.

[16] Gubser D U, Wolf S A and Cox J E “Shielding Of Longitudinal Magnetic Fields With Thin, Closely Spaced Concentric Cylinders Of High Permeability Material” REVIEW OF SCIENTIFIC INSTRUMENT VOL.50, PP. 751-756, 1979.